Decoupled UL/DL User Association in Wireless-Powered HetNets with Full-Duplex Small Cells

Sepideh Haghgoy, Mohammadali Mohammadi, *Member, IEEE,*
Zahra Mobini, *Member, IEEE,* and Kai-Kit Wong, *Fellow, IEEE*

***Abstract*—In this paper, we propose two downlink (DL)-uplink (UL) decoupled (DUDe) user association schemes in wireless-powered full-duplex (FD) heterogeneous networks (HetNets). We consider a two-tire HetNet comprising of half-duplex (HD) massive multi-antenna macrocell base stations (MBSs) and dual-antenna FD small cell base stations (SBSs) to support UL and DL transmissions of FD user equipments (UEs). Each FD UE is first associated to one MBSs/SBSs, based on the mean maximum received power (MMP) scheme or maximum received power (MRP) to harvest energy. During the consecutive data transmission phase, UEs choose to receive DL traffic from the same MBSs/SBSs as that associated with during energy harvesting phase, and send UL traffic through the same/another SBS. Leveraging tools from the stochastic geometry, we develop an analytical framework to analyze the average harvested energy and derive expressions for the UL and DL coverage probabilities of the proposed DUDe user association schemes. Our results show that there is an optimal value for the SBS density in the wireless-powered FD HetNets, at which both DL and UL coverage probabilities are maximized. Moreover, by applying MMPA and MRPA scheme, wireless-powered FD HetNets with DUDe achieves up to 138.78% and 83.37% energy efficiency gain over the FD HetNets with DL/UL coupled user association scheme and without wireless power transfer, respectively.**

***Index Terms*—Heterogeneous networks (HetNets), downlink-uplink decoupled (DUDe) user association, stochastic geometry.**

I. Introduction

The increasing prevalence of social media platform use has not only triggered an explosive increase in mobile data traffic demand, but also boosted the energy requirements to an unprecedented level. The evolution of social networking and cloud solutions has increased the priority weight of uplink (UL) transmissions in cellular networks compared to the traditional networks. To meet such requirements, full-duplex (FD)-enabled heterogeneous networks (HetNets) have been proposed to effectively enhance the UL and downlink (DL) spectral efficiency through the dense deployment of FD small-cell base stations (SBSs) [2]–[5]. The low-power nature of SBSs makes them an ideal host for the FD transceivers, as the self-interference (SI) becomes more manageable compared to the high-power macrocell base stations (MBSs) [2], [6]. Due to the difference between the UL and DL traffic loads expected in the next HetNets generation, it becomes essential to dynamically adjust UL/DL resources [7]. Moreover, by leveraging a massive number of SBSs in the macrocells and establishing the feasibility of intensive UL and DL transmissions, reduction of energy consumption is becoming a crucial aspect of such networks [8].

New proposed trend in cell association of DL/UL decoupling (DUDe) user association scheme along with wireless power transfer (WPT) in FD HetNets can offer substantial coverage and energy efficiency improvement over the half-duplex (HD) counterpart. DUDe breaks the constraint that user equipments (UEs) must be associated with the same base stations (BSs) in UL and DL [7], [9]. Therefore, UEs that are associated with a specific MBS in DL may prefer to access a geometrically closer SBS in UL for stronger signal strength and lower interference. WPT on the other hand, provides the potential of efficiently replenish the UEs batteries in the network by the means of microwave radio frequency (RF) signals [10]. WPT is mainly based on a "harvest-then-transmit" protocol [11], where self-sustainable devices first harvest energy in the DL and then transmit information in the UL [12], [13]. While DUDe user association and WPT are extensively discussed topics in the HetNet literature, their joint application has not been explored yet.

A. Related Works

1) FD HetNets and DUDe User Association: The performance of FD communication in HetNets has been studied in [2]–[5]. More specifically, the authors in [2] have provided a comprehensive modeling and analysis of two-tire HetNets with FD SBSs and HD MBSs using tools from stochastic geometry. The authors in [3] have established a foundation for hybrid-duplex HetNets, accounting for the spatial access points distribution, the SI cancellation capability, and the network interference. The authors in [4], have investigated the achievable spectral efficiency and association behavior of UEs and BSs in a two-tier HetNet, wherein the locations of all UEs and BSs are modeled using independent Poisson point processes (PPPs). A joint DL/UL beamforming design for discrete sum-rate maximization of the FD multicell HetNets has been proposed in [5].

DUDe user association in the FD HetNets has been studied in some prior works [14]–[20]. In [14], a simulation based study has been performed on two-tier HetNets, where the

S. Haghgoy, M. Mohammadi, Z. Mobini are with the Faculty of Engineering, Shahrekord University, Shahrekord 115, Iran (e-mails: haghgoy@stu.sku.ac.ir, {m.a.mohammadi, z.mobini}@sku.ac.ir).

K.-K. Wong is with the Department of Electronic and Electrical Engineering, University College London, London WC1E 6BT, U.K. (e-mail: kai-kit.wong@ucl.ac.uk).

Part of this work has been published at the 5th International Conference on Internet of Things and Applications (IoT 2021), Isfahan, Iran, May 2021 [1].

UL association is based on minimum path-loss, while the DL association is based on DL received power. The UL coverage probability of a two-tier random HetNet with DUDe user association has been studied in [15] and the gain of the DUDe user association over conventional DL/UL coupled (DUCo) user association scheme has been quantified. The authors in [16], proposed decoupled rate optimal user association scheme and then derived tight lower bounds on the maximum UL and DL rates of the FD links. In [17], resource allocation and user association were jointly optimized, and the performance of different resource allocation schemes and user association rules were analyzed. The authors in [18] developed a contract-theory based distributed approach for DUDe user association in FD HetNets. In [19], a joint dynamic time-division duplexing (TDD) and DUDe access statistical model was proposed based on a geometric probability approach to address UL and DL throughput degradation challenges. The authors in [20], investigated the performance of DUDe in device-to-device underlay HetNets, where a joint cell-association, subchannel allocation, and power control problem for UL sum-rate maximization has been studied.

2) WPT in HetNets: WPT has attracted increasing research attention in HetNets [12], [21]–[27]. The potential of WPT in massive multiple-input multiple-output (MIMO)-aided HetNets has been investigated in [12], where massive MIMO is applied in the MBSs, and UEs aim to harvest as much energy as possible and reduce the UL path-loss for enhancing their information transfer. In [21], a tractable analytical framework of K-tier HetNets with simultaneous wireless information and power transfer has been developed, where UEs harvest energy and decode information simultaneously in the DL, and then use harvested energy for UL information transmission. The work in [22], has focused on the wireless-powered millimeter wave HetNets and investigated the number of small cells that are required to achieve a targeted level of throughput. In [23], a multiuser two-tier HetNet with simultaneous wireless information and power transfer has been considered, where an energy efficiency (EE) maximization problem has been formulated and solved. By taking fairness into account, the authors in [24], have proposed a beamforming design problem in the simultaneous wireless information and power transfer HetNets. Energy harvesting in a cooperative HetNet with a dynamic sleeping strategy was investigated in [25], where the deactivated SBSs are cooperating with the rest of the network by harvesting then injecting the energy to the network. In [26], a Q-learning-based algorithm has been proposed to maximize the sum capacity in wireless-powered small cell HetNets. All aforementioned research [12], [21]–[27] primarily focus on HD HetNets. To the best of author's knowledge, the performance of DUDe user association in wireless-powered FD HetNets has not been investigated yet. To bridge this gap in the literature, in this paper, two DUDe user association schemes are proposed and analyzed in wireless-powered FD HetNets.

B. Motivation and Contribution

The main goal of this paper is to investigated $[R_1C_8]$ the UL/DL coverage probability and EE of DUDe user association in the wireless-powered FD HetNets. In order to implement WPT, each UE harvests energy from the dedicated RF signals transmitted from the serving BS (MBS/SBS) as well as ambient RF waves sent from other BSs in DL, and then utilizes the harvested energy for UL data transfer. Specifically, a two-tier HetNet consisting of macrocells and small cells is considered, where all the BSs and UEs are distributed according to the independent homogeneous PPPs. MBSs are HD enabled, each of which is equipped with massive antenna arrays and operates in DL, while SBSs are responsible for scheduling both UL and DL transmissions through the FD dual-antenna transceivers. The main contributions of this paper can be summarized as follows:

- In order to improve the network performance, interference management, and balanced distribution of UE's loads, two DUDe user association schemes are proposed. More specifically, each UE associates with a serving BS (MBS/SBS) based on the maximum mean receive power (MMP) or maximum receive power (MRP) for both DL WPT and data transmission, while it associates with the nearest SBS for UL transmissions.
- We exploit tools from stochastic geometry to characterize the average harvested energy in DL and to derive coverage probability expressions of the UL and DL transmissions for the proposed DUDe schemes. $[R_1C_8]$: We further investigate the EE performance of the system to quantify the merit of WPT in FD HetNets with DUDe.
- $[R_1C_2]$ $[R_2C_2]$: Our findings reveal that, compared to the HetNets with WPT and DUCo, by applying DUDe user association, coverage probability of the network is improved due to the fact that UL UEs are associated with serving BS based on minimum distance, thus the interference is reduced substantially. Moreover, by increasing SBS density, distance between UEs and SBSs decreases, thus the efficiency of DUDe increases. In addition, by reducing the energy harvesting time duration, the efficiency of DUDe is improved as the network interference is efficiently managed by controlling the UL transmit power of UEs.
- $[R_1C_2]$ $[R_2C_2]$: HetNet with WPT (under both DUDe and DUCo user association schemes) provides remarkable EE performance gains over the HetNets without WPT. This is because UE power consumption becomes lower than the case where UEs transmit with fixed power. As a result, interference caused by UEs can be managed more efficiently.
- Finally, by increasing the SBS density, UL coverage probability, achieved by MMPA and MRPA, increases first and then starts to decrease. Therefore, an optimal SBS density can be found, which yields the best UL coverage probability. This finding is in sharp contrast to the case of HetNets without WPT, where UL coverage probability is a monotonically decreasing function of the SBS density [2].

The rest of the paper is organized as follows: In section II, we describe the system model of the FD HetNet along

TABLE I: Notations

Parameter	Value
Φ_k, λ_k	k-th tier PPP and density
Φ_u, λ_u	UE PPP and density
P_M (P_S)	MBS (SBS) transmit power
$\mathtt{U}_0^{\mathtt{dl,M}}$, ($\mathtt{U}_0^{\mathtt{dl,S}}$)	Typical UE associated with MBS (SBS)
$\mathbf{h}_{M,i}$	channel between the MBS i and $\mathtt{U}_0^{\mathtt{dl,M}}$
$h_{S,i}$	channel between the SBS i and $\mathtt{U}_0^{\mathtt{dl,S}}$
$g^E_{M,0}$ ($g^E_{M,i}$)	Channel gain, serving (interfering) MBS and $\mathtt{U}_0^{\mathtt{dl,M}}$, WPT
$\bar{g}^E_{M,0}$	Channel gain, serving MBS and other UEs, WPT
$g^E_{S,0}$ ($g^E_{S,i}$)	Channel gain, serving (interfering) SBS and $\mathtt{U}_0^{\mathtt{dl,S}}$, WPT
$\bar{g}^E_{M,i}$	Channel gain, interfering MBSs and $\mathtt{U}_0^{\mathtt{dl,S}}$ in WPT
$\bar{g}^E_{S,i}$	Channel gain, interfering SBSs and $\mathtt{U}_0^{\mathtt{dl,M}}$ in WPT
$g^I_{M,0}$	Channel gain, serving MBS and $\mathtt{U}_0^{\mathtt{dl,M}}$, WIT
$g^I_{S,0}$	Channel gain, serving SBS and and $\mathtt{U}_0^{\mathtt{dl,S}}$, WIT
$g^I_{M,i}$ ($\bar{g}^I_{S,i}$)	Channel gain, interfering MBS (SBS) and $\mathtt{U}_0^{\mathtt{dl,M}}$ in WIT
$g^I_{S,i}$ ($\bar{g}^I_{M,i}$)	Channel gain, interfering SBS (MBS) and $\mathtt{U}_0^{\mathtt{dl,S}}$ in WIT
$h^U_{\mathtt{RSI}}$	Residual SI channel of $\mathtt{U}_0^{\mathtt{dl,S}}$ and $\mathtt{U}_0^{\mathtt{dl,M}}$
$h^S_{\mathtt{RSI}}$	Residual SI channel of the FD SBS
g_j	Channel gain, the typical SBS and the FD UEs
g_0	Channel gain, $\mathtt{U}_0^{\mathtt{dl,S}}$ and its serving SBS
$\beta_{M,i}$ ($\beta_{S,i}$)	Distance-dependent path-loss for the MBS (SBS) tier
α_M (α_S)	MBS (SBS) tier path-loss exponent
N	Number of MBS's antennas
K_d	Number of single-antenna UEs served by a MBS
T, τ	One block time and time allocation factor
$\mathbb{E}\{P_{U_0}\}$	Typical UE's transmit power
$\exp(\mu)$	Exponential distribution with mean μ
$\mathtt{Gamma}(\vartheta,\theta)$	Gamma distribution with shape ϑ and scale parameter θ

with the proposed DUDe users association schemes. In section III, we present the average power harvested at a typical UE and provide the UL/DL coverage probability analysis for the proposed DUDe user association schemes along with the EE performance. Numerical results and discussions are presented in section IV followed by the conclusion in Section V.

Notation: We use bold lower case letters to denote vectors; the superscript $(\cdot)^H$ stands for the conjugate-transpose; $|\cdot|$ denotes the absolute value of a complex scalar; $\|\cdot\|$ stands for Euclidean distance; $\mathrm{F}_X(\cdot)$ represents the cumulative distribution function (CDF) of a random variable (RV) X; $\mathrm{f}_X(\cdot)$ represents the probability density function (PDF) of a RV X; $\Pr(\cdot)$ denotes the probability; $\mathbb{E}\{\cdot\}$ denotes the statistical expectation; $\mathrm{Im}[\cdot]$ represents the imaginary part of the input complex argument. ${}_2F_1(\cdot,\cdot;\cdot;\cdot)$ is Gauss hypergeometric function [28, Eq. (9.111)]; $\Gamma(a,x)$ denotes Upper incomplete Gamma function [28, Eq. (8.350)]; $\Gamma(a)$ is Gamma function [28, Eq. (8.310)]. Table I lists some of the critical notations used in this article.

II. System Model

We consider a two-tier TDD-based HetNet, where the first tier consists of HD MBSs, and second tier comprises FD-enabled SBSs as shown in Fig. 1. MBSs, SBSs, and UEs are assumed to be distributed according to independent homogeneous PPPs. Let $\Phi_k \triangleq \{X_{k,i} \in \mathbb{R}^2 : i \in \mathbb{N}_+\}$ denotes the PPP for BSs with density λ_k, where $X_{k,i}, k \in \{M,S\}$, represents BS i in the k-th tier and its location, $\Phi_u \triangleq \{U_j \in \mathbb{R}^2 : j \in \mathbb{N}_+\}$ represents the PPP for UEs with density λ_u, and U_j denotes UE j and its location. Each HD MBS is

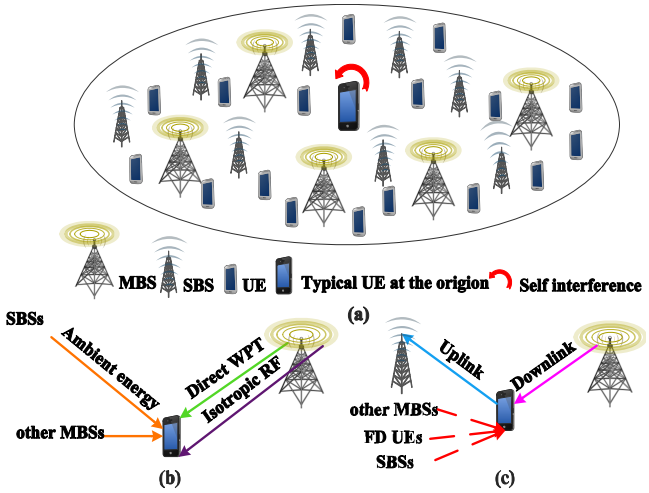

Fig. 1: (a) An illustration of a two-tier HetNet with FD small-cells, (b) Typical UE associated with MBS during energy harvesting, (c) Typical UE associated with SBS and MBS during information transmission phase.

equipped with N antennas and serves K_d single-antenna UEs in DL. Moreover, each small cell has one FD BS, equipped with two antennas, to serves both UL and DL transmissions over the same frequency band and at the same time.[1] The MBS and SBS transmit power are P_M and P_S, respectively, where $P_M > P_S$. [R_1C_6]: UEs operate in FD mode to simultaneously transmit and receive information over the same frequency band.[2]

A. DUDe User Association

To cope with the challenges raised by the network densification (including UEs and SBSs) and to improve the UL coverage, DUDe users association is applied in the network as depicted in Fig. 1. In particular, an FD UE U can associate with a BS ℓ in the UL but with a different BS ℓ' in the DL. In each time slot, each UE first harvests energy from the received signal of the serving BS (MBS/SBS) in DL and then uses the harvested energy to send UL traffic to the serving SBS. We recall that each FD UE can only associate with FD SBS for UL transmissions, while for DL transmission it can communicate with MBS or SBS. Therefore, due to the DUDe user association criterion, there are three sets of FD UEs: 1) UEs associate with MBS in the DL and SBS in the UL, 2) UEs associate with one SBS in DL and another SBS in UL, 3) UEs associate to the same SBS in DL and UL.

[1] It is assumed that the density of UEs is much greater than that of BSs so that there always will be one active UE at each time slot in every small cell and hence multiple active UEs in every macrocell [12].

[2] [R_1C_6]: System model can be further generalized to consider both FD and HD UEs in the network. Note that the mode of operation for different UEs are independent and depend on UEs' traffic. Let Φ_u^{FD} and $\Phi_u^{\mathsf{HD}} = \Phi_u - \Phi_u^{\mathsf{FD}}$ be the point processes of the FD and HD UEs, and are obtained by applying independent thinning on the PPP Φ_u using the transmission mode probability p_{FD} to determine whether an UE is operating in FD or HD. The intensities of Φ_u^{FD} and Φ_u^{HD} are respectively determined by $p_{\mathsf{FD}}\lambda_u$ and $(1-p_{\mathsf{FD}})\lambda_u$. This assumption changes the sources of the interference in the network. Therefore, we require a new performance analysis framework, which is set aside for our future work.

A general user association strategy to BS in DL/UL can be expressed as [29]–[31]

$$X^* = \arg \Psi^*(\|X^*\|) = \arg \sup_{k,i:X_{k,i}\in\Phi_k} \Psi_{k,i}(\|X_{k,i}\|), \quad (1)$$

where $\|X\|$ is the Euclidean distance from node X to a typical UE, $\Psi_{k,i}$ is the user association function of BS $X_{k,i}$, $\Psi^*(\cdot) \in \{\Psi_{k,i}, k \in \{M, S\}, i \in \mathbb{N}_+\}$ is the user association function of BS X^*. All $\Psi_{k,i}$'s are assumed to be monotonic and bijective decreasing functions. The following power-law-based function is commonly used as the user association function $\Psi_{k,i}(\cdot)$ for BS $X_{k,i}$

$$\Psi_{k,i}(x) = \frac{\psi_{k,i}}{x^{\alpha_k}}, \quad (2)$$

where $\psi_{k,i}$ is the k-th tier random bias and α_k is the path-loss exponent. The user association scheme in (2) can cover any distance-based cell association scheme.

1) DL user association: During the energy harvesting phase, UEs are associated to BSs according to MMP association (MMPA) or MRP association (MRPA) scheme and harvest energy. Accordingly, each UE will receive information from the the same BS (as energy serving BS) during the consecutive phase of information transfer in DL. Hereafter, we denote the typical UE associated with SBS and MBS for energy harvesting and DL transmissions by $\mathtt{U}_0^{\mathtt{dl,S}}$ and $\mathtt{U}_0^{\mathtt{dl,M}}$, respectively.

MMPA scheme: According to this user association scheme, UEs associate to serving BS based on MMP, i.e., $\psi_{k,i} = P_k$, where P_k is the transmit power of the k-th tier BS. Therefore, we get $\Psi_{k,i}(\|X_{k,i}\|) = P_k\|X_{k,i}\|^{-\alpha_k}$. In this case, the generalized user association scheme is termed as MMPA [30], [31].

MRPA scheme: For the second DL user association scheme, UE associates with the serving BS based on $\psi_{k,i} = P_k h_{k,i}$, where $h_{k,i}$ is the channel (power) gain between UE and its serving BS $X_{k,i}$. Therefore, we have $\Psi_{k,i}(\|X_{k,i}\|) = P_k h_{k,i}\|X_{k,i}\|^{-\alpha_k}$ that makes UEs associate with a BS that provides them with the maximum received power. In this case, the generalized user association scheme is called the MRPA [29], [30].

2) UL user association: For the UL user association, we consider the nearest BS association (NBA) scheme [2], [32]. Note that for the UL transmission, the UEs can only associate with the FD SBSs. In this scheme, $\psi_{S,i} = 1$ and thus we have $\Psi_{S,i}(\|X_{S,i}\|) = \|X_{S,i}\|^{-\alpha_S}$, that only characterizes the path-loss between SBS $X_{S,i}$ and typical UE U_0.

B. Signal Transmission Model

We assume that the communication block time is T and WPT time-splitting factor is τ, $0 < \tau < 1$. In the first τT subslot, called energy harvesting phase, the UE harvests power from the serving BS. In the second $(1-\tau)T$ subslot, called UL/DL information transmission phase, UEs upload information packet to BS by utilizing the harvested power and simultaneously download information packet from the BSs. $[R_1C_4]$ $[R_1C_5]$: Throughout this paper, we consider a block fading scenario, where the channels remain constant during each transmission block, but change independently from one block to the next [2], [12]. Let, the channel vector between the MBS i (the index of the serving MBS is set to $i = 0$), located at $X_{M,i}$, and $\mathtt{U}_0^{\mathtt{dl,M}}$ is denoted by $\sqrt{\beta_{M,i}}\mathbf{h}_{M,i}$, where $\mathbf{h}_{M,i} \in \mathbb{C}^{N\times 1}$ defines the small-scale Rayleigh channel fading with $\mathcal{CN}(0,1)$ independent and identically distributed (i.i.d.) components and $\beta_{M,i}$ is distance-dependent path-loss coefficient. Moreover, the channel vector between the SBS i (the index of the serving SBS is set to $i = 0$), and $\mathtt{U}_0^{\mathtt{dl,S}}$ is denoted by $\sqrt{\beta_{S,i}}h_{S,i}$, where $h_{S,i} \sim \mathcal{CN}(0,1)$ is the small-scale Rayleigh channel fading and $\beta_{S,i}$ is distance-dependent path-loss coefficient. We consider a standard path-loss model [21], i.e, $\beta_{M,i} = \|X_{M,i}\|^{-\alpha_M}$ ($\beta_{S,i} = \|X_{S,i}\|^{-\alpha_S}$), where $X_{M,i}$ ($X_{S,i}$) denotes the distance between serving MBS (SBS) and typical UE, and α_M (α_S) is the path-loss exponent for the macrocell (small cell) channel.

1) Energy harvesting phase: For wireless energy harvesting, all RF signals are exploited as energy sources. Therefore, in the massive MIMO macrocell, we adopt the simple linear maximum-ratio transmit (MRT) beamforming to direct RF signal toward intended UEs, $\mathtt{U}_0^{\mathtt{dl,M}}$. $[R_1C_4]$: By applying the MRT at the serving MBS as $\mathbf{w}_{M,0}^{\mathtt{MRT}} = \frac{\mathbf{h}_{M,0}}{\|\mathbf{h}_{M,0}\|}$, the channel gain between serving MBS and $\mathtt{U}_0^{\mathtt{dl,M}}$ is obtained as $g_{M,0}^E = |\mathbf{h}_{M,0}^H \mathbf{w}_{M,0}^{\mathtt{MRT}}|^2 \sim \mathtt{Gamma}(N,1)$.[3] Moreover, $\bar{g}_{M,0}^E \sim \mathtt{Gamma}(1,1)$ denotes fading channel power gain when the serving MBS directly transfers energy to other users in the same cell [12], and the channel gain between the interfering MBSs and $\mathtt{U}_0^{\mathtt{dl,M}}$ is denoted by $[R_2C_3]$ $g_{M,i}^E \sim \mathtt{Gamma}(1,1)$. Accordingly, during τ fraction of each time slot, the total harvested power at a typical UE, $\mathtt{U}_0^{\mathtt{dl,M}}$, that is associated with the serving MBS is given by (3) at the top of the next page. where $\mu = \frac{\eta\tau}{1-\tau}$, while $0 < \eta < 1$ is the RF-to-DC conversion efficiency; $P_{M,0}^1$ is the power harvested from the directed WPT of the serving MBS; $P_{M,0}^2$ is the power harvested from the isotropic RF signals; and $P_{M,0}^3$ is the power harvested from the ambient RF signals. The first term of $P_{M,0}^2$ is the harvested power from the interfering MBSs and the second term is the harvested power from the interfering SBSs, where $\bar{g}_{S,i}^E \sim \mathtt{Gamma}(1,1)$ and $X_{S,i}$ denote the small-scale fading gain of interfering channel and the distance between $\mathtt{U}_0^{\mathtt{dl,M}}$ and interfering SBS, respectively.

In each WPT subslot, the total harvested power at a typical UE associated with the serving SBS, i.e., $\mathtt{U}_0^{\mathtt{dl,S}}$, is given by

$$P_{S,0} = \mu\Bigg(\underbrace{P_S g_{S,0}^E \|X_{S,0}\|^{-\alpha_S}}_{P_{S,0}^1} + \underbrace{\sum_{X_{M,i}\in\Phi_M} P_M \bar{g}_{M,i}^E \|X_{M,i}\|^{-\alpha_M} + \sum_{X_{S,i}\in\Phi_S\setminus X_{S,0}} P_S g_{S,i}^E \|X_{S,i}\|^{-\alpha_S}}_{P_{S,0}^2}\Bigg), \quad (4)$$

where $P_{S,0}^1$ is the power harvested from the directed WPT of the serving SBS; $P_{S,0}^2$ is the power harvested from the ambient RF signals; $g_{S,0}^E \sim \mathtt{Gamma}(1,1)$ is the effective channel power gain between serving SBS, $X_{S,0}$, and $\mathtt{U}_0^{\mathtt{dl,S}}$. Furthermore, the first and second term of $P_{S,0}^2$ are the harvested power from interfering MBSs, $X_{M,i}$, and the harvested power from the

[3]Hereafter, we use subscript E and I in the related variables to denote the WPT and WIT phases, respectively.

$$P_{M,0}=\mu\Bigg(\underbrace{\frac{P_M}{K_d}g^E_{M,0}\|X_{M,0}\|^{-\alpha_M}}_{P^1_{M,0}}+\underbrace{\frac{(K_d-1)P_M}{K_d}\bar{g}^E_{M,0}\parallel X_{M,0}\parallel^{-\alpha_M}}_{P^2_{M,0}}+\underbrace{\sum_{X_{M,i}\in\Phi_M\setminus X_{M,0}}P_M g^E_{M,i}\parallel X_{M,i}\parallel^{-\alpha_M}+\sum_{X_{S,i}\in\Phi_S}P_S\bar{g}^E_{S,i}\parallel X_{S,i}\parallel^{-\alpha_S}}_{P^3_{M,0}}\Bigg), \tag{3}$$

interfering SBSs, $X_{S,i}$, where $g^E_{S,i}$ ($\bar{g}^E_{M,i}$) denotes the channel between interfering SBSs (MBSs) and $\mathtt{U}_0^{\mathtt{dl,S}}$.

2) Uplink/downlink information transmission phase: After energy harvesting, during the remaining $(1-\tau)$ fraction of each time slot, each MBS transmits K_d data streams to associated DL UEs using linear zero-forcing beamforming (ZFBF) with equal transmit power allocation [2]. ZFBF is applied at the MBS to spatially multiplex its K_d UEs, while suppressing interference on others, known as inter-beam interference.[4] Let $\mathbf{w}^{\mathtt{ZF}}_{M,0}$ denote ZF precoder associated with $\mathtt{U}_0^{\mathtt{dl,M}}$. The DL signal-to-interference-plus-noise ratio (SINR) at $\mathtt{U}_0^{\mathtt{dl,M}}$, serving by MBS, can be written as

$$\mathtt{SINR}^{\mathtt{dl}}_{\mathtt{M}}=\frac{\frac{P_M}{K_d}\beta g^I_{M,0}\parallel X_{M,0}\parallel^{-\alpha_M}}{\mathtt{I}_{\mathtt{U}_0^{\mathtt{dl,M}}}+P^{\mathtt{U}}_{\mathtt{RSI}}+N_0}, \tag{5}$$

$[R_1C_4]$: where $g^I_{M,0}=|\mathbf{h}^H_{M,0}\mathbf{w}^{\mathtt{ZF}}_{M,0}|\sim\mathtt{Gamma}\,(N-K_d+1,1)$ is the small-scale fading channel power gain between MBS $X_{M,0}$ and $\mathtt{U}_0^{\mathtt{dl,M}}$ [21], [33], β is the frequency dependent constant value; $P^{\mathtt{U}}_{\mathtt{RSI}}=\mathbb{E}\{P_{U_0}\}\Big|^i_M h^U_{\mathtt{RSI}}$ is the residual SI power after performing cancellation, where $h^U_{\mathtt{RSI}}\sim\mathtt{Gamma}(1,\sigma^2_{SI})$ is the residual SI channel of $\mathtt{U}_0^{\mathtt{dl,M}}$, where σ^2_{SI} denote the SI channel power gain [34], [35]. Moreover, $\mathtt{I}_{\mathtt{U}_0^{\mathtt{dl,M}}}=\mathtt{I}^{\mathtt{dl}}_{\mathtt{M}}+\mathtt{I}^{\mathtt{dl}}_{\mathtt{U}}$ is the aggregate interference at $\mathtt{U}_0^{\mathtt{dl,M}}$, where $\mathtt{I}^{\mathtt{dl}}_{\mathtt{M}}$ is interference from other BSs, given by

$$\mathtt{I}^{\mathtt{dl}}_{\mathtt{M}}=\mathtt{I}^{\mathtt{dl}}_{\mathtt{M,i}}+\mathtt{I}^{\mathtt{dl}}_{\mathtt{S,i}}, \tag{6}$$

with $\mathtt{I}^{\mathtt{dl}}_{\mathtt{M,i}}$ and $\mathtt{I}^{\mathtt{dl}}_{\mathtt{S,i}}$ are the interference caused by simultaneous DL transmission of other MBSs and SBSs, which are respectively expressed as

$$\mathtt{I}^{\mathtt{dl}}_{\mathtt{M,i}}=\sum_{X_{M,i}\in\Phi_M/X_{M,0}}P_M\beta g^I_{M,i}\|X_{M,i}\|^{-\alpha_M}, \tag{7a}$$

$$\mathtt{I}^{\mathtt{dl}}_{\mathtt{S,i}}=\sum_{X_{S,i}\in\Phi_S}P_S\beta\bar{g}^I_{S,i}\|X_{S,i}\|^{-\alpha_S}. \tag{7b}$$

Furthermore, $\mathtt{I}^{\mathtt{dl}}_{\mathtt{U}}$ is interference caused by the UL transmissions of other UEs, given by

$$\mathtt{I}^{\mathtt{dl}}_{\mathtt{U}}=\sum_{U_j\in\Phi_u\setminus U_0}\mathbb{E}\left\{P_{U_j}\right\}\beta g_j\|U_j\|^{-\alpha_S}. \tag{8}$$

In (7a), (7b), and (8) $[R_2C_3]$ $g^I_{M,i}\sim\mathtt{Gamma}(1,1)$, $\bar{g}^I_{S,i}\sim\mathtt{Gamma}(1,1)$, and $g_j\sim\mathtt{Gamma}(1,1)$ denote the small-scale fading channel power gain between $\mathtt{U}_0^{\mathtt{dl,M}}$ and the interfering MBSs, the interfering SBSs, the other FD UEs, respectively, while their corresponding distances are denoted as $X_{M,i}$, $X_{S,i}$, and U_j, respectively.

The DL SINR for a typical UE, located at the origin and associated to a SBS (termed as $\mathtt{U}_0^{\mathtt{dl,S}}$), can be written as

$$\mathtt{SINR}^{\mathtt{dl}}_{\mathtt{S}}=\frac{P_S\beta g^I_{S,0}\parallel X_{S,0}\parallel^{-\alpha_s}}{\mathtt{I}_{\mathtt{U}_0^{\mathtt{dl,S}}}+P^{\mathtt{U}}_{\mathtt{RSI}}+N_0}, \tag{9}$$

where $g^I_{S,0}\sim\mathtt{Gamma}(1,1)$ is the small-scale fading channel power gain between SBS $X_{S,0}$ and $\mathtt{U}_0^{\mathtt{dl,S}}$; $P^{\mathtt{U}}_{\mathtt{RSI}}=\mathbb{E}\{P_{U_0}\}\Big|^i_S h^U_{\mathtt{RSI}}$ is the residual SI power after performing SI cancellation, where $h^U_{\mathtt{RSI}}\sim\mathtt{Gamma}(1,\sigma^2_{SI})$ is the residual SI channel of $\mathtt{U}_0^{\mathtt{dl,S}}$ [34], [35]. Moreover, $\mathtt{I}_{\mathtt{U}_0^{\mathtt{dl,S}}}=\mathtt{I}^{\mathtt{dl}}_{\mathtt{S}}+\mathtt{I}^{\mathtt{dl}}_{\mathtt{U}}$ is the aggregate interference at $\mathtt{U}_0^{\mathtt{dl,S}}$, where $\mathtt{I}^{\mathtt{dl}}_{\mathtt{U}}$ is given in (8), and $\mathtt{I}^{\mathtt{dl}}_{\mathtt{S}}$ is interference from other BSs, given by

$$\mathtt{I}^{\mathtt{dl}}_{\mathtt{S}}=\mathtt{I}^{\mathtt{dl}}_{\mathtt{M,i}}+\mathtt{I}^{\mathtt{dl}}_{\mathtt{S,i}}, \tag{10}$$

with $\mathtt{I}^{\mathtt{dl}}_{\mathtt{M,i}}$ and $\mathtt{I}^{\mathtt{dl}}_{\mathtt{S,i}}$ are the interference caused by simultaneous DL transmission of MBSs and other SBSs, which are respectively expressed as

$$\mathtt{I}^{\mathtt{dl}}_{\mathtt{M,i}}=\sum_{X_{M,i}\in\Phi_M}P_M\beta\bar{g}^I_{M,i}\|X_{M,i}\|^{-\alpha_M}, \tag{11a}$$

$$\mathtt{I}^{\mathtt{dl}}_{\mathtt{S,i}}=\sum_{X_{S,i}\in\Phi_S/X_{S,0}}P_S\beta g^I_{S,i}\|X_{S,i}\|^{-\alpha_S}, \tag{11b}$$

where $\bar{g}^I_{M,i}\sim\mathtt{Gamma}(1,1)$ ($g^I_{S,i}\sim\mathtt{Gamma}(1,1)$) denotes the channel gain between interfering MBS (SBS) and $\mathtt{U}_0^{\mathtt{dl,S}}$ during the WPT phase.

The received UL SINR at a typical SBS located at the origin can be written as

$$\mathtt{SINR}^{\mathtt{ul}}_{\mathtt{S},0}=\frac{\mathbb{E}\{P_{U_0}\}\Big|^i_k\beta g_0\|U_0\|^{-\alpha_S}}{\mathtt{I}^{\mathtt{ul}}_{\mathtt{S},0}+P^{S}_{\mathtt{RSI}}+N_0}, \tag{12}$$

where $g_0\sim\mathtt{Gamma}(1,1)$ and U_0 are the small-scale fading channel power gain and distance between typical UE and its serving SBS $X_{S,o}$ respectively, and $P^S_{\mathtt{RSI}}=P_S h^S_{\mathtt{RSI}}$ is the residual SI power after performing cancellation, where $h^S_{\mathtt{RSI}}\sim\mathtt{Gamma}(1,\sigma^2_{SI})$ is the residual SI channel of the typical SBS [34], [35]. Moreover, $\mathtt{I}^{\mathtt{ul}}_{\mathtt{S},0}=\mathtt{I}^{\mathtt{ul}}_{\mathtt{S}}+\mathtt{I}^{\mathtt{ul}}_{\mathtt{U}}$ is the aggregate interference at typical SBS, where $\mathtt{I}^{\mathtt{ul}}_{\mathtt{S}}$ is the interference from other BSs

$$\mathtt{I}^{\mathtt{ul}}_{\mathtt{S}}=\mathtt{I}^{\mathtt{ul}}_{\mathtt{M,i}}+\mathtt{I}^{\mathtt{ul}}_{\mathtt{S,i}}, \tag{13}$$

where $\mathtt{I}^{\mathtt{ul}}_{\mathtt{M,i}}$ and $\mathtt{I}^{\mathtt{ul}}_{\mathtt{S,i}}$ denote the interference from MBSs and the other SBSs, given by

$$\mathtt{I}^{\mathtt{ul}}_{\mathtt{M,i}}=\sum_{X_{M,i}\in\Phi_M}P_M\beta g^I_{M,i}\|X_{M,i}\|^{-\alpha_M}, \tag{14a}$$

$$\mathtt{I}^{\mathtt{ul}}_{\mathtt{S,i}}=\sum_{X_{S,i}\in\Phi_S\setminus U_0}P_S\beta g^I_{S,i}\|X_{S,i}\|^{-\alpha_S}, \tag{14b}$$

respectively. $\mathtt{I}^{\mathtt{ul}}_{\mathtt{U}}$ is the interference due to the UL transmission of other UEs, given by

$$\mathtt{I}^{\mathtt{ul}}_{\mathtt{U}}=\sum_{U_j\in\Phi_u\setminus U_0}\mathbb{E}\left\{P_{U_j}\right\}g_j\beta\|U_j\|^{-\alpha_S}. \tag{15}$$

[4] $[R_1C_3]$: To fully eliminate the inter-beam interference via ZFBF, perfect CSI is needed at the BS. The perfect CSI can be accomplished by advanced channel estimation strategy with adequate training data to guarantee perfect CSI at the MBSs [2]. Orthogonal pilot sequence is sent by each UE to the MBS during the training phase, where it is properly estimated by the MBS without pilot contamination. As a result, the MBSs and UEs have access to the perfect CSI. Nevertheless, perfect CSI is not always achievable in some practical scenarios due to estimation error, quantized feedback, or channel mobility. Imperfect CSI yields inaccurate ZFBF designs, which then translates to inter-beam interference. However, we leave such a design and its analysis as interesting future work.

In (14a), (14b), and (15) $g^I_{M,i} \sim \texttt{Gamma}(1,1)$, $g^I_{S,i} \sim \texttt{Gamma}(1,1)$, and $g_j \sim \texttt{Gamma}(1,1)$ denote the small-scale fading channel power gain between the typical SBS and the MBSs, the SBSs, and the FD UEs, respectively, and their corresponding distances are denoted as $X_{M,i}$, $X_{S,i}$, and U_j, respectively.

III. Performance Evaluation

In this section, we analyze the coverage probability of two-tier HetNet with FD small cells. Coverage probability is a metric that represents the average fraction of the cell area that is in coverage at any time [2]. We define the coverage probability as the probability that the instantaneous SINR of a randomly located UE is larger than a SINR threshold. To derive the coverage probability, the average UL power transfer needs to be first characterized.

A. Average Uplink Power Transfer Analysis

The UL transmit power of a typical UE in the k-th tier is required for the UL coverage probability analysis. Therefore, we determine the average received power at the typical UE $\texttt{U}_0^{\texttt{dl,k}}$ according to the MMPA and MRPA scheme.

Lemma 1: With MMPA and MRPA scheme, the average received power at the $\texttt{U}_0^{\texttt{dl,M}}$ is given by

$$\mathbb{E}\{P_{U_0}\}\Big|^i_M = \mu 2\pi\lambda_M \left(P_M \left(\Upsilon \Xi_1 + \frac{2\pi\lambda_M}{\alpha_M - 2} \Xi_2 \right) + \frac{2\pi\lambda_S}{\alpha_S - 2} P_S \Xi_3 \right), \tag{16}$$

where $i \in \{\texttt{MMPA}, \texttt{MRPA}\}$, $\Upsilon = \frac{N+K_d-1}{K_d}$ and

$$\Xi_1 = \int_0^{x_0} \frac{x^{1-\alpha_M}}{\Lambda^i_M} \exp\left(-\pi\lambda_S \left(\frac{P_S}{\delta_i P_M} \right)^{\frac{2}{\alpha_S}} x^{\frac{2\alpha_M}{\alpha_S}} - \pi\lambda_M x^2 \right) dx,$$

$$\Xi_2 = \int_{x_0}^{\infty} \frac{x^{3-\alpha_M}}{\Lambda^i_M} \exp\left(-\pi\lambda_S \left(\frac{P_S}{\delta_i P_M} \right)^{\frac{2}{\alpha_S}} x^{\frac{2\alpha_M}{\alpha_S}} - \pi\lambda_M x^2 \right) dx,$$

$$\Xi_3 = \int_{x_0}^{\theta_i} \frac{x\theta_i^{2-\alpha_S}(x)}{\Lambda^i_M} \exp\left(-\pi\lambda_S \left(\frac{P_S}{\delta_i P_M} \right)^{\frac{2}{\alpha_S}} x^{\frac{2\alpha_M}{\alpha_S}} - \pi\lambda_M x^2 \right) dx,$$

with $\delta_{\texttt{MMPA}} = \frac{1}{K_d}$, [$R_1C_7$] $\delta_{\texttt{MRPA}} = \Upsilon$; x_0 denote lowest distance between a typical UE and serving BS; $\theta_{\texttt{MMPA}}(x) = \left(\frac{K_d P_S}{P_M} \right)^{\frac{1}{\alpha_S}} x^{\frac{\alpha_M}{\alpha_S}}$ and $\theta_{\texttt{MRPA}}(x) = \left(\frac{P_S}{\Upsilon P_M} \right)^{\frac{1}{\alpha_S}} x^{\frac{\alpha_M}{\alpha_S}}$ are the distance between the closest interfering MBS and the typical UE, respectively; Λ^i_M, Λ^i_S denote the probability that a typical UE is associated with MBS and SBS, and are given as [12]

$$\Lambda^i_M = 2\pi\lambda_M \int_0^{\infty} r \exp\left(-\pi\lambda_S \left(\frac{P_S}{\delta_i P_M} \right)^{\frac{2}{\alpha_S}} r^{\frac{2\alpha_M}{\alpha_S}} - \pi\lambda_M r^2 \right) dr, \tag{17a}$$

$$\Lambda^i_S = 2\pi\lambda_S \int_0^{\infty} r \exp\left(-\pi\lambda_M \left(\frac{\delta_i P_M}{P_S} \right)^{\frac{2}{\alpha_M}} r^{\frac{2\alpha_S}{\alpha_M}} - \pi\lambda_S r^2 \right) dr, \tag{17b}$$

respectively.

Proof 1: See Appendix B. [R_1C_{11}]

Lemma 2: With MMPA and MRPA scheme, the average received power at the $\texttt{U}_0^{\texttt{dl,S}}$ can be expressed as

$$\mathbb{E}\{P_{U_0}\}\Big|^i_S = \mu 2\pi\lambda_S \left(P_S \left(\Xi_4 + \frac{2\pi\lambda_S}{\alpha_S - 2} \Xi_5 \right) + \frac{2\pi\lambda_M}{\alpha_M - 2} P_M \Xi_6 \right), \tag{18}$$

where $i \in \{\texttt{MMPA}, \texttt{MRPA}\}$ and

$$\Xi_4 = \int_0^{x_0} \frac{x^{1-\alpha_S}}{\Lambda^i_S} \exp\left(-\pi\lambda_M \left(\frac{\delta_i P_M}{P_S} \right)^{\frac{2}{\alpha_M}} x^{\frac{2\alpha_S}{\alpha_M}} - \pi\lambda_S x^2 \right) dx,$$

$$\Xi_5 = \int_{x_0}^{\infty} \frac{x^{3-\alpha_S}}{\Lambda^i_S} \exp\left(-\pi\lambda_M \left(\frac{\delta_i P_M}{P_S} \right)^{\frac{2}{\alpha_M}} x^{\frac{2\alpha_S}{\alpha_M}} - \pi\lambda_S x^2 \right) dx,$$

$$\Xi_6 = \int_{x_0}^{\ell_i} \frac{x\ell_i^{2-\alpha_M}(x)}{\Lambda^i_S} \exp\left(-\pi\lambda_M \left(\frac{\delta_i P_M}{P_S} \right)^{\frac{2}{\alpha_M}} x^{\frac{2\alpha_S}{\alpha_M}} - \pi\lambda_S x^2 \right) dx,$$

while $\ell_{\texttt{MMPA}}(x) = \left(\frac{P_M}{K_d P_S} \right)^{\frac{1}{\alpha_M}} x^{\frac{\alpha_S}{\alpha_M}}$ and $\ell_{\texttt{MRPA}}(x) = \left(\frac{\Upsilon P_M}{P_S} \right)^{\frac{1}{\alpha_M}} x^{\frac{\alpha_S}{\alpha_M}}$ are the distance between the closest interfering MBS and the typical UE, respectively.

Proof 2: The proof is similar to Lemma 1 and thus omitted for the sake of brevity.

Overall, the average received power at a UE in the network with $i \in \{\texttt{MMPA}, \texttt{MRPA}\}$ is given by

$$\mathbb{E}\{P_{U_0}\}^i = \Lambda^i_M \mathbb{E}\{P_{U_0}\}\Big|^i_M + \Lambda^i_S \mathbb{E}\{P_{U_0}\}\Big|^i_S. \tag{19}$$

To get more insights, we now turn our attention towards characterizing the average received power at the typical UE for the special case of $\alpha_M = \alpha_S = \alpha$.

Corollary 1: When $\alpha_M = \alpha_S = \alpha$, the average received power at the typical UE associated with the MBS based on MMPA/MRPA scheme reduces to

$$\mathbb{E}\{P_{U_0}\}\Big|^i_M = \mu P_M \left(\Upsilon \vartheta^{\frac{\alpha}{2}} \Gamma\left(1 - \frac{\alpha}{2}\right) + \frac{2\pi\lambda_M}{\alpha - 2} \vartheta^{\frac{\alpha}{2}-1} \times \Gamma\left(2 - \frac{\alpha}{2}\right) \right) + \mu P_S \frac{\pi^{\frac{3}{2}}\lambda_S}{\alpha - 2} \kappa_i \vartheta^{-\frac{1}{2}}, \tag{20}$$

where $\vartheta = \pi\lambda_M + \pi\lambda_S \left(\frac{P_S}{\delta_i P_M} \right)^{\frac{2}{\alpha}}$ and $\kappa_i = \left(\frac{P_S}{\delta_i P_M} \right)^{\frac{1}{\alpha}}$.

Corollary 2: When $\alpha_M = \alpha_S = \alpha$, the average received power at the typical UE associated with the SBS based on MMPA/MRPA scheme reduces to

$$\mathbb{E}\{P_{U_0}\}\Big|^i_S = \mu P_S \left(\varpi^{\frac{\alpha}{2}} \Gamma\left(1 - \frac{\alpha}{2}\right) + \frac{2\pi\lambda_S}{\alpha - 2} \varpi^{\frac{\alpha}{2}-1} \times \Gamma\left(2 - \frac{\alpha}{2}\right) \right) + \mu P_M \frac{\pi^{\frac{3}{2}}\lambda_M}{\alpha - 2} \varsigma_i \varpi^{-\frac{1}{2}}, \tag{21}$$

where $\varpi = \pi\lambda_M \left(\frac{\delta_i P_M}{P_S} \right)^{\frac{2}{\alpha}} + \pi\lambda_S$ and $\varsigma_i = \left(\frac{\delta_i P_M}{P_S} \right)^{\frac{1}{\alpha}}$.

Remark 1: For both MMPA and MRPA schemes, by increasing $\frac{\lambda_M}{\lambda_S}$, the probability that a UE is associating to the MBS is decreased. On the other hand, the probability that a UE is associated to the SBS is increased. Moreover, the received power at the typical UE, associated with MBS and SBS, is increased.

Remark 2: For both MMPA and MRPA schemes, by increasing the number of MBS antennas, N, the probability that a UE is associated to the MBS is increased and in turn the probability that a UE is associated to the SBS based on MRPA scheme is decreased. Moreover, the received power at the typical UE, associated with MBS based on MMPA and MRPA schemes, and SBS based on MRPA scheme is increased.

$$\mathtt{C}^{\mathtt{dl}}_{\mathtt{M,i}} = \frac{2\pi\lambda_M}{\Lambda^i_M}\int_0^\infty x\left(\frac{1}{2}\Big(\exp\left(-\pi\lambda_M x^2-\pi\lambda_S\theta_i^2\right)\Big)-\frac{1}{\pi}\int_0^\infty \mathrm{Im}\Bigg[\exp\Bigg(-jw\Big(\frac{\beta P_M}{\gamma_{\mathtt{mM}}x^{\alpha_M}}-N_0\Big)-\pi\lambda_M\Omega_{1,M}(x,w)$$
$$-2\pi\lambda_S\Big(\Omega_{2,M}(x,w)+\Omega_3\Big)-\pi\lambda_M x^2-\pi\lambda_S\theta_i^2\Bigg)\frac{1}{1-jw\epsilon\sigma^2_{SI}\mathbb{E}\left\{P_{U_0}\right\}\Big|^i_M}\Bigg]\frac{dw}{w}\Bigg)dx, \tag{24}$$

$$\mathtt{C}^{\mathtt{dl}}_{\mathtt{S,i}} = \frac{2\pi\lambda_S}{\Lambda^i_S}\int_0^\infty x\left(\frac{1}{2}\Big(\exp\left(-\pi\lambda_M\ell_i^2-\pi\lambda_S x^2\right)\Big)-\frac{1}{\pi}\int_0^\infty \mathrm{Im}\Bigg[\exp\Bigg(-jwN_0-\pi\lambda_M\Omega_{1,S}(x,w)$$
$$-2\pi\lambda_S\Big(\Omega_{2,S}(x,w)+\Omega_3\Big)-\pi\lambda_M\ell_i^2-\pi\lambda_S x^2\Bigg)\frac{1}{\left(1+\frac{jw\beta P_S}{\gamma_{\mathtt{th}}x^{\alpha_S}}\right)\left(1-jw\epsilon\sigma^2_{SI}\mathbb{E}\left\{P_{U_0}\right\}\Big|^i_S\right)}\Bigg]\frac{dw}{w}\Bigg)dx, \tag{25}$$

B. Downlink Coverage Probability Analysis

The DL coverage probability of a typical UE in the considered two-tier HetNet is given by

$$\mathtt{C}^{\mathtt{dl}}_{\mathtt{i}} = \sum_{\mathtt{k}\in\{\mathtt{M,S}\}}\Lambda^i_k\mathtt{C}^{\mathtt{dl}}_{\mathtt{k,i}}, \tag{22}$$

where Λ^i_k is the per-tier association probability based on MMPA/MRPA scheme ($i\in\{\mathtt{MMPA},\mathtt{MRPA}\}$) and $\mathtt{C}^{\mathtt{dl}}_{\mathtt{k,i}}$ is the coverage probability of a typical UE associated with k-th tier BSs.

Assuming that typical UE is located at the distance x from its serving BS (MBS/SBS) and $\gamma_{\mathtt{th}}=\frac{\gamma}{1-\tau}$, with γ is a SINR threshold, the DL coverage probability is given by

$$\mathtt{C}^{\mathtt{dl}}_{\mathtt{k,i}} = \mathbb{E}_x\left\{\Pr\left(\mathtt{SINR}^{\mathtt{dl}}_{\mathtt{k}}(x)\geq\gamma_{\mathtt{th}}\Big|x\right)\right\},\quad \mathtt{k}\in\{\mathtt{M,S}\}, \tag{23}$$

where $\mathtt{SINR}^{\mathtt{dl}}_{\mathtt{k}}$ is given in (5) or (9) .

Proposition 1: With MMPA/MRPA scheme, the DL coverage probability of a typical UE associated with the MBS is given by (24) at the top of the page, where Λ^i_M and $\mathbb{E}\left\{P_{U_0}\right\}\Big|^i_M$ are the probability that a typical UE is associated with MBS and the average power harvested at $\mathtt{U}^{\mathtt{dl,k}}_0$, and are given in (17a) and (16), respectively. Moreover, $\gamma_{\mathtt{mM}}=\frac{K_d\gamma_{\mathtt{th}}}{N-K_d+1}$, and

$$\Omega_{1,M}(x,w)=\frac{\Gamma\left(1-\frac{2}{\alpha_M}\right)+\frac{2}{\alpha_M}\Gamma\left(\frac{-2}{\alpha_M},\frac{-jw\beta P_M}{x^{\alpha_M}}\right)}{(-jw\beta P_M)^{\frac{2}{\alpha_M}}}-x^2,$$
$$\Omega_{2,M}(x,w)=\frac{-jw\beta P_S\theta_i^{2-\alpha_S}}{\alpha_S-2}{}_2F_1\left[1,1-\frac{2}{\alpha_S};2-\frac{2}{\alpha_S};\frac{jw\beta P_S}{\theta_i^{\alpha_S}}\right],$$
$$\Omega_3(w)=\frac{-1}{2}jw\mathbb{E}\left\{P_{U_0}\right\}^i\Gamma\left(1+\frac{2}{\alpha_S}\right)\Gamma\left(1-\frac{2}{\alpha_S}\right).$$

Proof 3: See Appendix C. [R_1C_{11}]

Proposition 2: With MMPA/MRPA scheme, the DL coverage probability of a typical UE associated with the SBS is given by (25) at the top of the page, where Λ^i_S and $\mathbb{E}\left\{P_{U_0}\right\}\Big|^i_S$ denote the probability that a typical UE is associated with SBS and the average harvested power at $\mathtt{U}^{\mathtt{dl,S}}_0$, given in (17b) and (18), respectively, $\Omega_3(x,w)$ is given in Proposition 1, and

$$\Omega_{1,S}(x,w)=\frac{\Gamma\left(1-\frac{2}{\alpha_M}\right)+\frac{2}{\alpha_M}\Gamma\left(\frac{-2}{\alpha_M},\frac{-jw\beta P_M}{(\ell_i)^{\alpha_M}}\right)}{(-jw\beta P_M)^{\frac{2}{\alpha_M}}}-(\ell_i)^2,$$
$$\Omega_{2,S}(x,w)=\frac{-jw\beta P_S x^{2-\alpha_S}}{\alpha_S-2}{}_2F_1\left[1,1-\frac{2}{\alpha_S};2-\frac{2}{\alpha_S};\frac{jw\beta P_S}{x^{\alpha_S}}\right].$$

Proof 4: The proof is similar to Proposition 1 and thus omitted for the sake of brevity.

C. Uplink Coverage Probability Analysis

The coverage probability for a typical UE associated with SBS, $\mathtt{C}^{\mathtt{ul}}_{\mathtt{S}}$, can be written as

$$\mathtt{C}^{\mathtt{ul}}_{\mathtt{S}} = \mathbb{E}_{\|U_0\|}\left\{\Pr\left(\mathtt{SINR}^{\mathtt{ul}}_{\mathtt{S,0}}(\|U_0\|)\geq\gamma_{\mathtt{th}}\Big|\|U_0\|\right)\right\}, \tag{26}$$

where $\mathtt{SINR}^{\mathtt{ul}}_{\mathtt{S,0}}$ is given in (12).

Proposition 3: The UL coverage probability for a typical UE associated with SBS based on NBA scheme is given by (27) at the top of the next page, where $i\in\{\mathtt{MMPA},\mathtt{MRPA}\}$, $k\in\{\mathtt{M,S}\}$ for MBS and SBS, and

$$\xi_1(x,w)=\frac{\Gamma\left(1-\frac{2}{\alpha_M}\right)+\frac{2}{\alpha_M}\Gamma\left(-\frac{2}{\alpha_M},\frac{-jw\beta P_M}{R^{\alpha_M}}\right)}{(-jw\beta P_M)^{\frac{2}{\alpha_M}}}-R^2,$$
$$\xi_2(x,w)=\frac{-jw\beta P_S R^{2-\alpha_S}}{\alpha_S-2}{}_2F_1\left[1,1-\frac{2}{\alpha_S};2-\frac{2}{\alpha_S};\frac{jw\beta P_S}{R^{\alpha_S}}\right],$$
$$\xi_3(w)=\frac{-1}{2}jw\mathbb{E}\left\{P_{U_0}\right\}^i\Gamma\left(1+\frac{2}{\alpha_S}\right)\Gamma\left(1-\frac{2}{\alpha_S}\right).$$

Proof 5: See Appendix D. [R_1C_{11}]

Therefore, the UL coverage probability of a random UE in the network is given by

$$\mathtt{C}^{\mathtt{ul}}_{\mathtt{i}} = \sum_{\mathtt{k}\in\{\mathtt{M,S}\}}\Lambda^i_k\mathtt{C}^{\mathtt{ul,DUDe}}_{\mathtt{k,i}}, \tag{28}$$

where $k\in\{\mathtt{M,S}\}$ and $i\in\{\mathtt{MMPA},\mathtt{MRPA}\}$, $\mathtt{C}^{\mathtt{ul,DUDe}}_{\mathtt{k,i}}$ is the UL coverage probability for $\mathtt{U}^{\mathtt{dl,k}}_0$.

As benchmark for comparison, we provide the UL coverage probability of the DUCo user association in the following Proposition.

Proposition 4: The UL coverage probability for a typical UE associated with SBS based on DUCo user association is given by (29) at the top of the next page, where $\xi_4=-\pi\lambda_M\left(\frac{\delta_i P_M}{P_S}\right)^{\frac{2}{\alpha_M}}x^{\frac{2\alpha_S}{\alpha_M}}-\pi\lambda_S x^2$ and

$$\mathtt{C}_{\mathtt{k,i}}^{\mathtt{ul,DUDe}} = 2\pi\lambda_S \int_0^\infty x \left[\frac{1}{2}\Big(\exp\left(-\pi\lambda_S x^2\right)\Big) - \frac{1}{\pi}\int_0^\infty \mathrm{Im}\left[\exp(-jwN_0 - \pi\lambda_M \xi_1(x,w) - 2\pi\lambda_S\Big(\xi_2(x,w) + \xi_3(x,w)\Big)\pi\lambda_S x^2\right) \left(1 + \frac{jw\beta\mathbb{E}\left\{P_{U_0}\right\}\Big|_k^i}{\gamma_{\mathtt{th}} x^{\alpha_S}}\right)^{-1} \left(1 - jw\epsilon\sigma_{SI}^2 P_S\right)^{-1}\right]\frac{dw}{w}\right] dx, \quad (27)$$

$$\mathtt{C}_{\mathtt{S,i}}^{\mathtt{ul,DUCo}} = \frac{2\pi\lambda_S}{\Lambda_S^i}\int_0^\infty x\left[\frac{1}{2}\exp\Big(-\xi_{4,k}(x)\Big) - \frac{1}{\pi}\int_0^\infty \mathrm{Im}\left[\exp\Big(-jwN_0 - \pi\lambda_M\xi_5(x,w) - 2\pi\lambda_S\Big(\xi_6(x,w) + \xi_7(w)\Big) - \xi_{4,k}(x)\Big)\left(1 + \frac{jw\beta\mathbb{E}\left\{P_{U_0}\right\}\Big|_S^i}{\gamma_{\mathtt{th}}x^{\alpha_S}}\right)^{-1}\left(1 - jw\epsilon\sigma_{SI}^2 P_S\right)^{-1}\right]\frac{dw}{w}\right]dx, \quad (29)$$

$$\mathtt{C}_{\mathtt{M,i}}^{\mathtt{dl}} = \frac{1}{2} - 2\lambda\left(1 + \left(\frac{P_S}{\delta_i P_M}\right)^{\frac{2}{\alpha}}\right) \times \left(\int_0^\infty\int_0^\infty x\,\mathtt{Im}\left[\exp\left(-j\omega\left(\frac{\beta P_M}{\gamma_{\mathtt{mM}}x^\alpha} - N_0\right) - 2\pi\lambda\left(\frac{1}{2}\left(\Omega_{1,M}(x,\omega) + x^2 + \theta_i^2\right) + \Omega_{2,M}(x,\omega) + \Omega_3(\omega)\right)\right)\right]\frac{d\omega}{\omega}dx\right), \quad (30)$$

$$\xi_5(x,w) = \frac{\Gamma\left(1 - \frac{2}{\alpha_M}\right) + \frac{2}{\alpha_M}\Gamma\left(-\frac{2}{\alpha_M}, \frac{-jw\beta P_M}{R^{\alpha_M}}\right)}{(-jw\beta P_M)^{\frac{2}{\alpha_M}}} - R^2,$$

$$\xi_6(x,w) = \frac{-jw\beta P_S R^{2-\alpha_S}}{\alpha_S - 2}\,{}_2F_1\left[1, 1 - \frac{2}{\alpha_S}; 2 - \frac{2}{\alpha_S}; \frac{jw\beta P_S}{R^{\alpha_S}}\right],$$

$$\xi_7(w) = \frac{-1}{2}jw\mathbb{E}\left\{P_{U_0}\right\}^i \Gamma\left(1 + \frac{2}{\alpha_S}\right)\Gamma\left(1 - \frac{2}{\alpha_S}\right).$$

Proof 6: See Appendix E. $[R_1C_{11}]$

Remark 3: $[R_3C_4]$: Although the coverage probability expressions in (24), (25), (27), and (29) are not simple enough to provide immediate insight, but they are general and fast to evaluate using popular scientific software packages such as MATLAB and Mathematica.

Corollary 3: $[R_3C_4]$ Under MMPA and MRPA DUDe user association schemes, when $\alpha_M = \alpha_S = \alpha$, $\lambda_M = \lambda_S = \lambda$, by considering perfect SI cancellation at the FD UE, DL coverage probability for a typical UE associated with MBS in (24) reduces to (30) at the top of the page, where $i \in \{\mathtt{MMPA}, \mathtt{MRPA}\}$. Likewise, DL coverage probability for a typical UE, associated with SBS reduces to (31) at the top of the next page, where $i \in \{\mathtt{MMPA}, \mathtt{MRPA}\}$.

Remark 4: By inspecting (30) and (31), it can be readily found that in dense FD WPT-enabled HetNets with $\lambda_M = \lambda_S = \lambda \to \infty$, $\mathtt{C}_{\mathtt{k,i}}^{\mathtt{dl}} \to \frac{1}{2}$, $k \in \{\mathtt{M}, \mathtt{S}\}$ and $i \in \{\mathtt{MMPA}, \mathtt{MRPA}\}$. This is because the interference dominant the gains achieved by decreasing the distance between UEs and BSs. While reducing the distances over which data and power transfers are made improves both efficiency of WPT and accuracy of data detection during WIT, the transmit power of the UL UEs as well as interference between the BSs increase. This finding raises the necessity of applying functionalities such as power control and interference management in dense FD HetNets with WPT.

Corollary 4: Assuming $\alpha_M = \alpha_S = \alpha$, $\lambda_M = \lambda_S = \lambda$, and perfect SI cancellation at the SBS, UL coverage probability for $\mathtt{U}_0^{\mathtt{dl,k}}$ in (27) reduces to (32) at the top of the nest page. Moreover, it can be readily checked that, when $\lambda \to \infty$ then $\mathtt{C}_{\mathtt{k,i}}^{\mathtt{ul,DUDe}} \to \frac{1}{2}$.

D. $[R_3C_2]$ Energy Efficiency

In this subsection, we study the EE of the WPT-enabled FD HetNet with DUDe, to quantify the merit of the WPT in FD HetNets. We recall that the EE of the WPT-enabled network can be defined as

$$\mathtt{EE}_{\mathtt{WPT}} = \frac{\mathtt{ASE}}{\mathtt{P}_{\mathtt{c}}^{\mathtt{WPT}}} \quad (33)$$

where $\mathtt{ASE} = \lambda_S \mathtt{C}_{\mathtt{i}}^{\mathtt{ul}} \log(1+\gamma_{\mathtt{th}})$ is the area spectral efficiency, where $\mathtt{C}_{\mathtt{i}}^{\mathtt{ul}}$, $i \in \{\mathtt{MMPA}, \mathtt{MRPA}\}$, has been given in (28). Moreover, $\mathtt{P}_{\mathtt{c}}^{\mathtt{WPT}}$ denotes the average network power consumption, which is given by [36], [37]

$$\mathtt{P}_{\mathtt{c}}^{\mathtt{WPT}} = \lambda_S \zeta \mathbb{E}\left\{P_{U_0}\right\}^i + P_{\mathtt{fix}}, \quad (34)$$

where $\mathbb{E}\left\{P_{U_0}\right\}^i$ is given by (19), and $P_{\mathtt{fix}}$ is the circuit power consumption and ζ is the power amplifier efficiency.

On the other hand, the EE for UL transmission in HetNet without WPT can be obtained as

$$\mathtt{EE} = \frac{\lambda_S \bar{\mathtt{C}}_{\mathtt{i}}^{\mathtt{ul}} \log(1+\gamma)}{\mathtt{P}_{\mathtt{c}}}, \quad (35)$$

where $\bar{\mathtt{C}}_{\mathtt{i}}^{\mathtt{ul}}$ denote UL coverage probability for a random UE in the HetNet without WPT which has been given in (27), in which $\mathbb{E}\left\{P_{U_0}\right\}^i$ is replaced by P_u, where P_u is the fixed transmit power of each UEs, and average power consumption, $\mathtt{P}_{\mathtt{c}}$ is

$$\mathtt{P}_{\mathtt{c}} = \lambda_S \zeta P_u + P_{\mathtt{fix}}. \quad (36)$$

$$\mathtt{C}_{\mathtt{S,i}}^{\mathtt{dl}} = \frac{1}{2} - 2\lambda \left(1+\left(\frac{\delta_i P_M}{P_S}\right)^{\frac{2}{\alpha}}\right) \times \left(\int_0^\infty \int_0^\infty x \mathtt{Im}\left[\exp\left(-j\omega N_0 - 2\pi\lambda\left(\frac{1}{2}\Omega_{1,S}(x,\omega) + \Omega_{2,S}(x,\omega) + \Omega_3(\omega) + \frac{1}{2}\left(x^2+\ell_i^2\right)\right)\right)\right]\frac{d\omega}{\omega}dx\right). \quad (31)$$

$$\mathtt{C}_{\mathtt{k,i}}^{\mathtt{ul,DUDe}} = \frac{1}{2} - 2\lambda \int_0^\infty \int_0^\infty \mathrm{Im}\left[\frac{\exp\left(-jwN_0 - 2\pi\lambda\frac{1}{2}\left(\xi_1(x,w)+x^2\right)+\xi_2(x,w)+\xi_3(w)\right)}{1+\frac{jw\beta\mathbb{E}\left\{P_{U_0}\right\}\Big|_k^i}{\gamma_{\mathrm{th}}x^{\alpha_S}}}\right]\frac{dw}{w}dx. \quad (32)$$

TABLE II: System's parameters.

Parameter	Value	Parameter	Value
P_M	40 dBm	P_S	33 dBm
α_M	3.5	α_S	4
β, η	0.9	τ	0.6
ζ	0.38	N_0	-100 dBm
P_u	23 dBm	P_{fix}	100 mW

IV. Numerical Results and Discussion

In this section, we investigate the impact of different user association schemes and system parameters on the average harvested power, UL/DL coverage probability, and EE of the two-tier HetNet with FD small cells. The analytical results are confirmed by Monte Carlo simulation for Poisson randomly position of MBSs, SBSs, and UEs according to their densities λ_M, λ_S, and λ_u, respectively, where $\lambda_u \geq K_d\lambda_M + \lambda_S$. We performed system level simulations, where BSs and UEs deployed in a circular area with radius $[R_1C_9]$ $R_a = 100$ km^2 and $\lambda_M = 10^{-3}$ km^{-2} using random geometry tools $[R_1C_9]$ [2], [12]. The simulation results are accomplished by averaging over 10^5 realizations in MATLAB. Unless otherwise stated, the system's parameters used in this section are listed in Table II.

Fig. 2a and Fig. 2b compare the user association probability of the typical UE with the serving MBS, Λ_M^i, and SBS, Λ_S^i with $i \in \{\mathtt{MMPA}, \mathtt{MRPA}\}$, for different MBS power levels, P_M and different MBS antenna number N, respectively. Opposite trends for Λ_M^i and Λ_S^i are observed with the increase of λ_S/λ_M. More specifically, by increasing λ_S/λ_M, the user association probability to the serving MBS is decreased, while the association probability to the serving SBS is increased. This is intuitive, since UEs tend to associate with BS tiers with larger deployment intensity as the access distance is shorter, which yields lower path-loss. This in turn increases the available SBSs for the UE to associate with. Therefore, for fixed number of MBSs, when λ_S increases the UEs are more likely to associated with the SBSs rather than the MBSs. In Fig. 2, we also observe that when the MBS transmit power, P_M, is increased, Λ_M^i increases while Λ_S^i decreases. This can be explained by the fact that in both proposed user association schemes, UEs tend to associate with the BS tires which provide more power in DL. Furthermore, the same behavior can be observed by employment of more transmit antennas at the

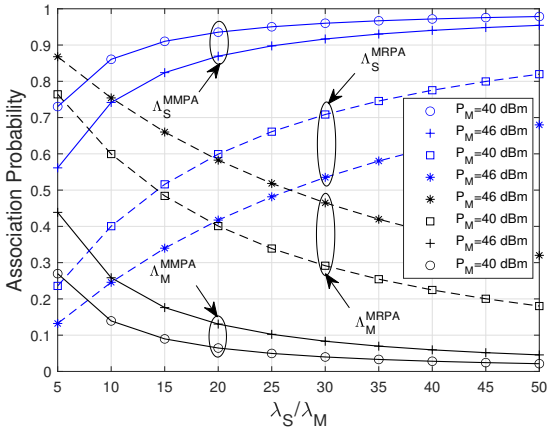

(a) The association probability for different power levels and for MMPA and MRPA schemes ($N = 64$).

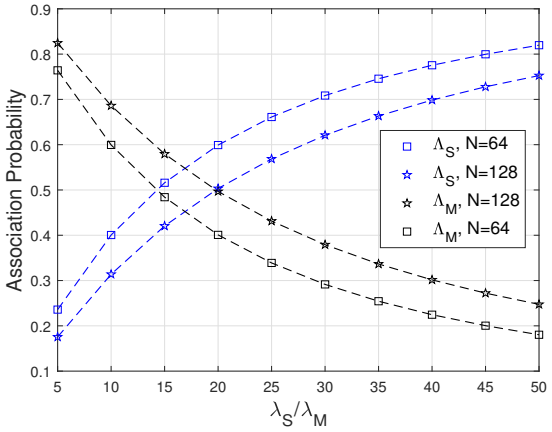

(b) The association probability for different MBS antenna number for MRPA scheme ($P_M = 40$ dBm).

Fig. 2: The association probability with serving MBS and SBS.

MBSs, N, as it improves the amount of received power at the DL UE.

Fig. 3a and Fig. 3b compare average power harvested at the typical DL UE associated with MBS, (16), and SBSs (18), and for MMPA and MRPA schemes, respectively. It can be noticed that when λ_S/λ_M increases, the amount of harvested power with both association schemes increases at both tiers. Moreover, increasing the number of antennas at the MBS

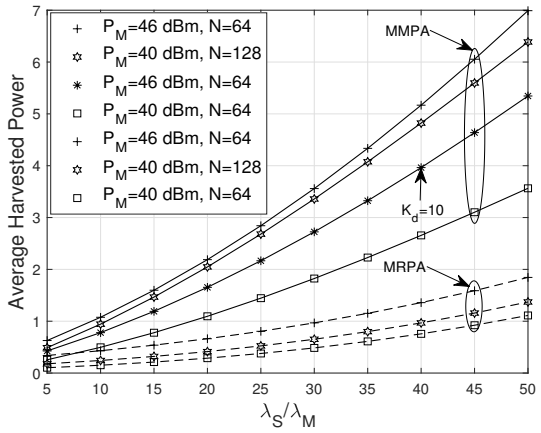

(a) The average harvested power at UE, associated with MBS and SBS for MRPA scheme ($K_d = 5$).

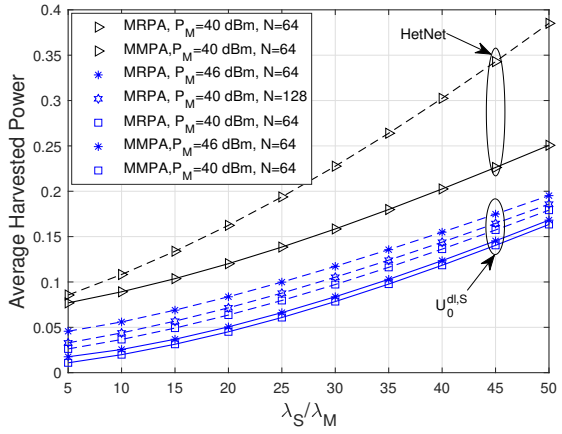

(b) The average harvested power at UE, associated with MBS ($N = 64$, $P_M = 40$ dBm).

Fig. 3: Average harvested power at a typical UE.

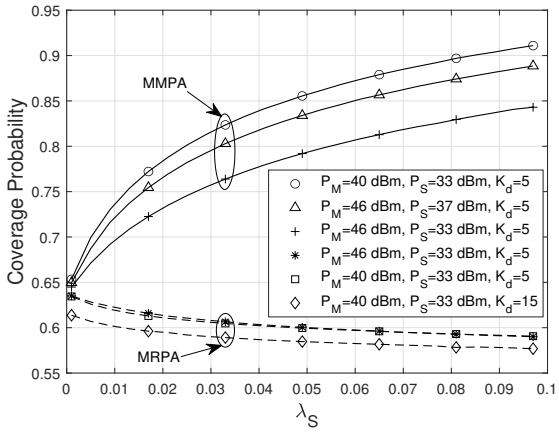

Fig. 4: DL coverage probability for a typical UE, associated with MBS.

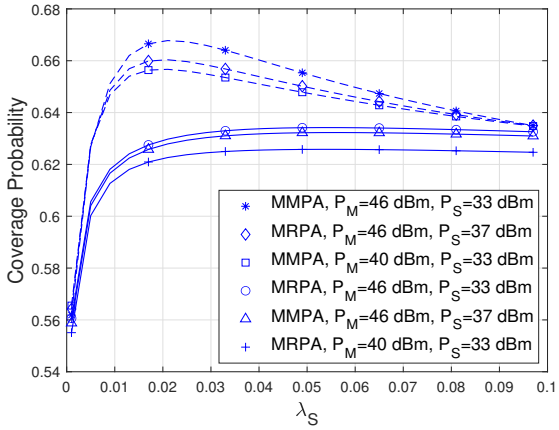

Fig. 5: DL coverage probability for a typical UE associated with SBS.

improves the efficiency of MRPA scheme not only in the first tier but also in second tier. This is due to the fact that by adding more antennas at the MBSs, UEs with low received power are offloaded to MBSs. However, the average harvested power for both MMPA and MRPA schemes at both tiers, with the increasing power of MBS increases because of rising harvested power from direct and ambient sources. From Fig. 3a, it is clear that UEs associated with MBS, harvest more power with the MMPA scheme than the MRPA scheme. Moreover, for MMPA schemes, by decreasing the number of serving UEs at the MBSs, i.e., K_d, the amount of harvested power from direct and ambient RF increases. This can be interpreted as the MBS will use the same amount of power to serve less number of UEs, which in turn improves the received power at the UEs (i.e., $\frac{P_M}{K_d}$ is increased). From Fig. 3b, we observe that as expected MRPA outperforms MMPA scheme in the FD HetNet.

Fig. 4 examines the effect of λ_S on DL coverage probability of the typical UE associated with MBS, $\mathtt{U}_0^{\mathtt{dl,M}}$, based on MMPA and MRPA schemes. The solid and dashed lines show analytical results, derived using (24) while marked points are obtained using Monte Carlo simulations. It can be readily noticed that the DL coverage probability of the MMPA scheme increases rapidly and reaches a maximum value at $\lambda_S^* \approx 0.1$. The reason is that, by increasing the SBS's density distance between SBSs and UEs are shortened and, accordingly, the received power at the UEs and association probability Λ_S^i increases. Therefore, the UEs are offload towards SBSs instead of MBSs and consequently, the interference from the SBSs decreases. Thus, the DL coverage probability is increased. Finally, it is observed that the DL coverage probability with MRPA decreases by increasing λ_S. This is due to the fact that when λ_S increases average UEs harvested power increases thus the received interference from UL UEs increased. In addition, coverage probability with MMPA is much better than MRPA. This is because Λ_M^i decreases when λ_S increases (Please see Fig. 2a). Hence, transmit power of the MBSs, i.e., $\frac{P_M}{K_d}$ increases which subsequently improves the DL coverage probability.

Fig. 5 shows DL coverage probability of a typical UE associated with SBS, $\mathtt{U}_0^{\mathtt{dl,S}}$, versus λ_S for different levels of MBSs and SBSs transmit power. We consider the same setting as in Fig. 4. The DL coverage probability for MMPA and MRPA schemes have the same behavior; it first increases to reach the local maximum at $\lambda_S \approx 0.05$ and ≈ 0.01 for MMPA and MRPA, respectively, and then decreases. Because increasing λ_S decreases distance between UEs and SBSs, thus

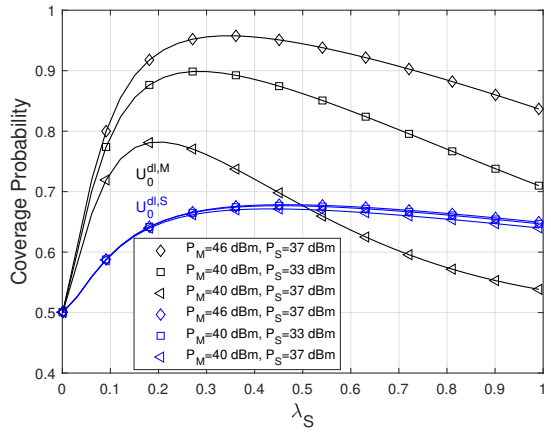

Fig. 6: UL coverage probability versus λ_S ($K_d = 15$).

the DL coverage probability is increased, whereas, at high λ_S, coverage probability decreases due to increasing intra-cell interference. Moreover, DL coverage probability based on the MRPA outperforms the MMPA. With MRPA and MMPA scheme, by increasing P_M from 40 dBm to 46 dBm (for fixed $P_S = 33$ dBm) DL coverage is improved, while by increasing P_S from 33 dBm to 37 dBm (for fixed $P_M = 46$ dBm) DL coverage probability is degraded over all values of λ_S. It shows that increasing the P_k of the k-th tier has a minor effect on DL coverage probability, and increasing P_k cannot significantly improve DL coverage probability because both DL user association schemes rely on the power of the both tiers.

Fig. 6 shows the UL coverage probability of the typical UEs, $\mathtt{U}_0^{\mathtt{dl,M}}$ and $\mathtt{U}_0^{\mathtt{dl,S}}$, which are associated with the MBSs and SBSs during the energy harvesting phase and for DL transmissions, respectively. We recall that UL transmissions of both $\mathtt{U}_0^{\mathtt{dl,M}}$ and $\mathtt{U}_0^{\mathtt{dl,S}}$ are served by the SBSs as the MBSs are HD-enabled and only operate in DL. It is clear that, there exists an optimal value for the SBS density λ_S, which provides the maximum UL coverage probability for $\mathtt{U}_0^{\mathtt{dl,M}}$ or $\mathtt{U}_0^{\mathtt{dl,S}}$. By increasing λ_S the UL performance of the $\mathtt{U}_0^{\mathtt{dl,M}}$ is more degraded compared to the $\mathtt{U}_0^{\mathtt{dl,S}}$. Moreover, we observe that increasing the P_S or decreasing the P_M causes the performance degradation.

$[R_1C_{10}]$ $[R_2C_4]$: In Fig. 7, we examine the impact of MBS and UE density on the DL and UL coverage probability of the proposed MRPA scheme and for different values of σ_{SI}^2. As expected, by increasing the strength of the SI, the DL and UL coverage performance of the system are degraded. Moreover, when λ_U/λ_M is small, SI causes more degradation in DL and UL coverage probability. This is because, SI dominates the interference from other BSs and UEs in low UE density regime. Furthermore, we observe that when SI is efficiently cancelled (i.e., for sufficiently small values of σ_{SI}^2), DL coverage probability of both tiers reduces by increasing λ_U/λ_M, due to increases in interference from UL UEs. Fig. 7b shows that, when λ_U/λ_M grows large, the UL coverage probability increases, reaches the maximum value and then decreases under both weak and strong SI strength regimes. This is due to the fact that, when the UE density is increased, distance between UEs and SBSs decreases and the UL coverage probability is improved. However, by increasing λ_U/λ_M beyond the optimum value, the number of interferers increases, leading to the UL coverage probability degradation. Moreover, we observe that when $\sigma_{SI}^2 \to 0$, the UL coverage probability is remarkably improved over the all λ_U/λ_M values, which demonstrates the necessity of SI cancellation.

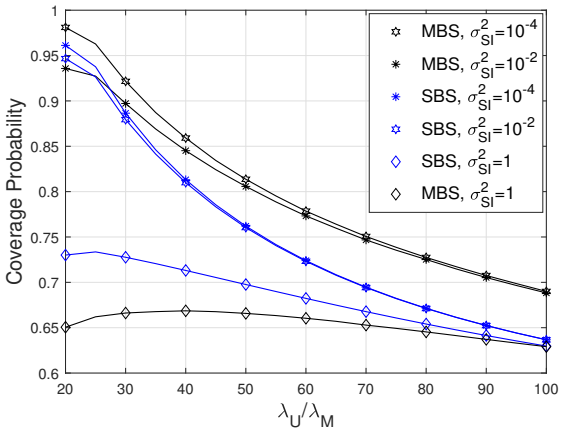

(a) DL coverage probability.

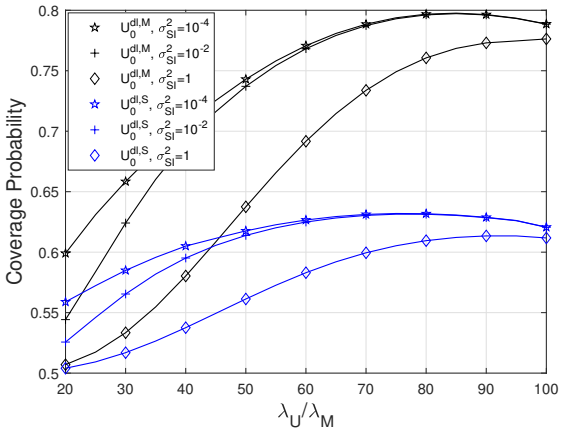

(b) UL coverage probability.

Fig. 7: Coverage probability for a typical UE versus λ_U/λ_M ($P_M = 40$ dBm, $P_S = 37$ dBm, $K_d = 5$, $N = 64$)

$[R_3C_2]$: Fig. 8 compares the EE performance of the considered system with the following benchmarks: 1) HetNet without WPT and under DUDe user association (**DUDe, without WPT**), 2) HetNet without WPT and under DUCo user association (**DUCo, without WPT**), 3) HetNet with WPT and DUCo (**DUCo, WPT**). From this figure, we observe that the EE of the HetNets with WPT and DUDe is significantly improved over the **DUCo, WPT**, **DUDe, without WPT**, and **DUCo, without WPT**. More specifically, with MMPA scheme and when $\lambda_S = 0.25$, the relative EE gain achieved by enabling WPT and DUDe in HetNets is up to 138.78% and 83.37% over the **DUCo, without WPT**, for MMPA and MRPA scheme, respectively. This observation demonstrates the merits of applying WPT and DUDe in the FD HetNets. Moreover, it is clear that MMPA outperforms the MRPA, and the gains achieved by the MRPA are disappeared by increasing λ_S and τ.

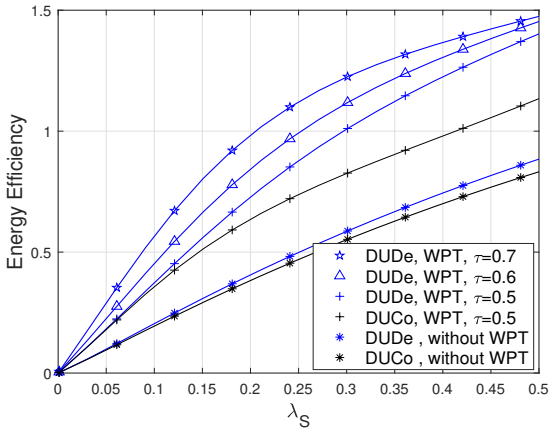

(a) MMPA

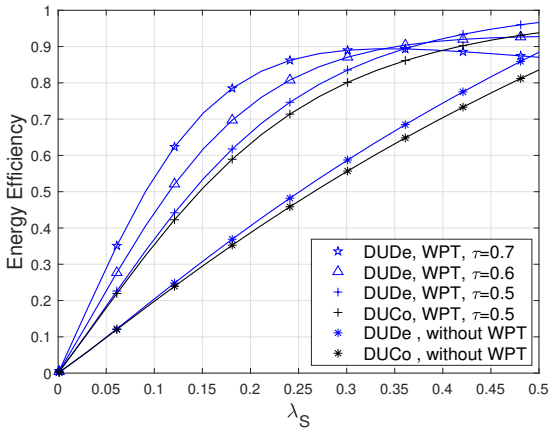

(b) MRPA

Fig. 8: Comparing Energy Efficiency in different HetNet ($P_M = 40$ dBm, $P_S = 33$ dBm, $K_d = 5$).

V. Conclusion

In this paper, we investigated the performance of a two-tier HetNet with FD small cells with DUDe user association in terms of the average harvested energy, DL/UL coverage probability, and EE. In particular, we proposed two DL user association schemes, namely MMPA and MRPA schemes. We characterized, analytically using stochastic geometry, the DL coverage probability for macrocells and small cells and UL coverage probability for SBSs. Furthermore, we thoroughly investigated the impact of the system parameters, such as SBS's density, power of MBS, the number of MBS antennas, and SI strength on the UL and DL coverage probabilities. Numerical results have shown that there is an optimum value for the SBS density to improve the DL and UL coverage probabilities. Moreover, we found that the network performance in term of coverage probability and EE is significantly improved by applying DUDe user association as compared to the DUCo scheme.

Appendix A
Preliminary Results of Distance to Serving BS

In this Appendix, we present some useful results that are frequently invoked to derive key results.

Lemma 5 [2]: The pdf of the distance between a typical UE and its serving MBS in DL, is given by

$$f^i_{X_{M,0}}(x) = \frac{2\pi\lambda_M}{\Lambda^i_M} x \exp\left(-\pi\lambda_S \left(\frac{P_S}{\delta_i P_M}\right)^{\frac{2}{\alpha_S}} x^{\frac{2\alpha_M}{\alpha_S}} - \pi\lambda_M x^2\right), \tag{37}$$

where $i \in \{\texttt{MMPA}, \texttt{MRPA}\}$, and Λ^i_M is the probability that a typical DL UE is associated with MBS, which has been given in (17a).

Lemma 6 [2]: The pdf of the distance between a typical UE and its serving SBS in DL is given by

$$f^i_{X_{S,0}}(x) = \frac{2\pi\lambda_S}{\Lambda^i_S} x \exp\left(-\pi\lambda_M \left(\frac{\delta_i P_M}{P_S}\right)^{\frac{2}{\alpha_M}} x^{\frac{2\alpha_S}{\alpha_M}} - \pi\lambda_S x^2\right), \tag{38}$$

where Λ^i_S is the probability that a typical DL UE is associated with SBS, and has been given in (17b).

Lemma 7 [2]: With the NBA user association, the pdf of the distance between a typical UE and its serving SBS in UL is given by

$$f^{NBA}_{X_{S,0}}(x) = 2\pi\lambda_S x \exp\Big(-\pi\lambda_S x^2\Big). \tag{39}$$

Appendix B
Proof of Lemma1

The average power harvested at the typical UE, associated with MBS in DL for WPT, is given by

$$\mathbb{E}\left\{P_{U_0}\right\}\Big|^i_M = \int_0^\infty \widetilde{P}_{U_0}\Big|^i_M f^i_{X_{M,0}}(x)dx, \tag{40}$$

where $f^i_{X_{M,0}}(x)$ is the pdf of distance between the typical UE and its serving MBS, given in (37), and $\widetilde{P}_{U_0}\Big|^i_M$ is expressed by (41) at the top of the next page, where the last equality follows from the fact that $\mathbb{E}\{g^E_{M,0}\} = N$ and $\mathbb{E}\{\bar{g}^E_{M,0}\} = 1$. Additionally, the average power harvested from interfering MBS, i.e., second term of (41), can be calculated as

$$\mathbb{E}\Big\{\sum_{X_{M,i}\in\Phi_M\setminus X_{M,0}} P_M g^E_{M,i}\|X_{M,i}\|^{-\alpha_M}\Big\} =$$

$$2\pi\lambda_M P_M \int_x^\infty r^{-\alpha_M} r dr = 2\pi\lambda_M P_M \frac{x^{2-\alpha_M}}{\alpha_M - 2}, \tag{42}$$

where we used probability generating functional (PGFL) of the PPP to obtain the first equality and the fact that $g^E_{M,i} \sim \texttt{Gamma}(1,1)$. In (42), $X_{M,0} = x$ is the minimum distance between typical UE and the interfering MBS.

In addition, the third term in (41) which presents the average power harvested from interfering SBSs, is obtained as

$$\mathbb{E}\left\{\sum_{X_{S,i}\in\Phi_S} P_S \bar{g}^E_{S,i}\|X_{S,i}\|^{-\alpha_S}\right\} = 2\pi\lambda_S P_S \frac{\theta_i^{2-\alpha_S}}{\alpha_S - 2}, \tag{43}$$

where we used the PGFL of the PPP and then $\bar{g}^E_{S,i} \sim \texttt{Gamma}(1,1)$. In (43), θ_i is the nearest distance between the typical UE and SBS interferer. By substituting (43) and (42) into (41), we can rewrite $\widetilde{P}_{U_0}\Big|^i_M$ as

$$\widetilde{P}_{U_0}\Big|^i_M = \mu\left(\Upsilon P_M x^{-\alpha_M} + 2\pi\lambda_M P_M \frac{x^{2-\alpha_M}}{\alpha_M - 2} + 2\pi\lambda_S P_S \frac{\theta_i^{2-\alpha_S}}{\alpha_S - 2}\right), \tag{44}$$

Finally, plugging (44) into (40) we obtain (16).

$$\widetilde{P}_{U_0}\Big|_{M}^{i}=\mu\mathbb{E}\left\{\frac{P_M}{K_d}g_{M,0}^{E}\|X_{M,0}\|^{-\alpha_M}\right\}+\mu\mathbb{E}\left\{\frac{(K_d-1)P_M}{K_d}\bar{g}_{M,0}^{E}\|X_{M,0}\|^{-\alpha_M}\right\}$$
$$+\mu\mathbb{E}\left\{\sum_{X_{M,i}\in\Phi_M/X_{M,0}}P_M g_{M,i}^{E}\parallel X_{M,i}\parallel^{-\alpha_M}+\sum_{X_{S,i}\in\Phi_S}P_S\bar{g}_{S,i}^{E}\parallel X_{S,i}\parallel^{-\alpha_S}\right\}$$
$$=\mu\left(N+K_d-1\right)\frac{P_M}{K_d}x^{-\alpha_M}+\mu\mathbb{E}\left\{\sum_{X_{M,i}\in\Phi_M/X_{M,0}}P_M g_{M,i}^{E}\parallel X_{M,i}\parallel^{-\alpha_M}\right\}+\mu\mathbb{E}\left\{\sum_{X_{S,i}\in\Phi_S}P_S\bar{g}_{S,i}^{E}\parallel X_{S,i}\parallel^{-\alpha_S}\right\},\tag{41}$$

APPENDIX C
PROOF OF PROPOSITION1

By invoking (23), the DL coverage probability of a typical UE associated with the MBS can be expressed as

$$\mathtt{C}_{\mathtt{M,i}}^{\mathtt{dl}}=\int_0^\infty \Pr\left(\mathtt{SINR}_{\mathtt{M}}^{\mathtt{dl}}(x)\geq\gamma_{\mathtt{th}}\middle|\|X_{k,0}\|=x\right)f_{X_{M,0}}^{i}(x)dx$$
$$=\int_0^\infty \Pr\left(\frac{\frac{P_M}{K_d}\beta g_{M,0}^{I}x^{-\alpha_M}}{\mathtt{I}_{\mathtt{U}_0^{\mathtt{dl},\mathtt{M}}}+\epsilon P_{\mathtt{RSI}}^{\mathtt{U}}+N_0}\geq\gamma_{\mathtt{th}}\right)f_{X_{M,0}}^{i}(x)dx$$
$$=\int_0^\infty \Pr\left(\mathtt{I}_{\mathtt{U}_0^{\mathtt{dl},\mathtt{M}}}\leq\frac{P_M\beta g_{M,0}^{I}}{S\gamma_{\mathtt{th}}x^{\alpha_M}}-\epsilon P_{\mathtt{RSI}}^{\mathtt{U}}-N_0\right)f_{X_{M,0}}^{i}(x)dx$$
$$=\int_0^\infty F_{\mathtt{I}_{\mathtt{U}_0^{\mathtt{dl},\mathtt{M}}}}\left(\mathtt{I}_{\mathtt{U}_0^{\mathtt{dl},\mathtt{M}}}\leq\frac{P_M\beta\mathbb{E}\left\{g_{M,0}^{I}\right\}}{K_d\gamma_{\mathtt{th}}x^{\alpha_k}}-\epsilon P_{\mathtt{RSI}}^{\mathtt{U}}-N_0\right)f_{X_{M,0}}^{i}(x)dx,\tag{45}$$

where $\mathbb{E}\left\{g_{M,0}^{I}\right\}=N-K_d+1$, and $f_{X_{M,0}}^{i}(x)$ is the pdf of the distance between a typical UE and its serving MBS, given by (37). By applying the Gil-Pelaez inversion theorem [2] and using the cdf of the interference, we can obtain $F_{\mathtt{I}_{\mathtt{U}_0^{\mathtt{dl},\mathtt{M}}}}(\cdot)$ as

$$F_{\mathtt{I}_{\mathtt{U}_0^{\mathtt{dl},\mathtt{M}}}}(x)=\tag{46}$$
$$\frac{1}{2}-\frac{1}{\pi}\int_0^\infty \mathrm{Im}\left[\frac{\mathcal{L}_{\mathtt{I}_{\mathtt{M}}^{\mathtt{dl}}}(-jw)\cdot\mathcal{L}_{\mathtt{I}_{\mathtt{U}}^{\mathtt{dl}}}(-jw)}{\exp\left(jw\left(\frac{\rho P_M\beta}{\gamma_{\mathtt{mM}}x^{\alpha_M}}-\epsilon P_{\mathtt{RSI}}^{\mathtt{U}}-N_0\right)\right)}\right]\frac{dw}{w}.$$

In (46), due to the independence of the interfering channels, the Laplace transform of $\mathtt{I}_{\mathtt{M}}^{\mathtt{dl}}$ can be derived as

$$\mathcal{L}_{\mathtt{I}_{\mathtt{M}}^{\mathtt{dl}}}(-jw)=\mathcal{L}_{\mathtt{I}_{\mathtt{M,i}}^{\mathtt{dl}}}(-jw)\cdot\mathcal{L}_{\mathtt{I}_{\mathtt{S,i}}^{\mathtt{dl}}}(-jw),\tag{47}$$

where $\mathcal{L}_{\mathtt{I}_{\mathtt{M,i}}^{\mathtt{dl}}}(-jw)$ and $\mathcal{L}_{\mathtt{I}_{\mathtt{S,i}}^{\mathtt{dl}}}(-jw)$ are the Laplace transform of the pdf of $\mathtt{I}_{\mathtt{M,i}}^{\mathtt{dl}}$ and $\mathtt{I}_{\mathtt{S,i}}^{\mathtt{dl}}$, respectively. In (47), $\mathcal{L}_{\mathtt{I}_{\mathtt{M,i}}^{\mathtt{dl}}}(-jw)$ can be obtained as

$$\mathcal{L}_{\mathtt{I}_{\mathtt{M,i}}^{\mathtt{dl}}}(-jw)=\mathbb{E}\left\{e^{-(-jw)\mathtt{I}_{\mathtt{M,i}}^{\mathtt{dl}}}\right\}$$
$$=\mathbb{E}_{\Phi,h}\left\{\exp\left(\sum_{X_{M,i}\in\Phi_M/X_{M,0}}P_M g_{M,i}^{I}\beta\|X_{M,i}\|^{-\alpha_M}\right)\right\}$$
$$\overset{(a)}{=}\mathbb{E}_{\Phi}\left\{\prod_{X_{M,i}\in\Phi_M/X_{M,0}}\exp\left(jwP_M\beta\|X_{M,i}\|^{-\alpha_M}\right)\right\}$$
$$\overset{(b)}{=}\exp\left(-2\pi\lambda_M\int_x^\infty\left(1-\exp\left(jwP_M\beta x^{-\alpha_M}\right)\right)dx\right),\tag{48}$$

where (a) follows from $\mathbb{E}\left\{g_{M,i}^{I}\right\}=1$, (b) is obtained by using PGFL of the PPP, and x is the shortest distance between typical UE and interfering MBS. Likewise, the $\mathcal{L}_{\mathtt{I}_{\mathtt{S,i}}^{\mathtt{dl}}}(-jw)$ can be derived as

$$\mathcal{L}_{\mathtt{I}_{\mathtt{S,i}}^{\mathtt{dl}}}(-jw)=\exp\left(-2\pi\lambda_S\int_{\theta_i}^\infty\left(\frac{-jwP_S\beta x^{-\alpha_S}}{1-jwP_S\beta x^{-\alpha_S}}\right)xdx\right),\tag{49}$$

where we have used the fact that $\bar{g}_{S,i}^{I}\sim\mathtt{Gamma}(1,1)$, and θ_i is the distance between a typical UE and the closet interfering SBSs. Moreover,

$$\mathcal{L}_{\mathtt{I}_{\mathtt{U}}^{\mathtt{dl}}}(-jw)=\mathbb{E}\left\{\prod_{U_j\in\Phi_u/U_0}\exp\left(jw\mathbb{E}\{P_{U_j}\}g_j\beta\|U_j\|^{-\alpha_S}\right)\right\}$$
$$\overset{(a)}{=}\exp\left(-2\pi\lambda_S\Lambda_k^{i}\int_0^\infty\left(\frac{-jw\mathbb{E}\left\{P_{U_0}\right\}\Big|_k^i\beta u^{-\alpha_S}}{1-jw\mathbb{E}\left\{P_{U_0}\right\}\Big|_k^i\beta u^{-\alpha_S}}\right)udu\right),\tag{50}$$

where (a) represents the density of the FD UEs depends on the serving BS in DL and $g_j\sim\mathtt{Gamma}(1,1)$.

To this end, by substituting (50) into (46), and then plugging (46) into (45), we obtain the desired result in (24).

APPENDIX D
PROOF OF PROPOSITION3

By invoking (12) and (26), the UL coverage probability for a typical UE ($\mathtt{U}_0^{\mathtt{dl,k}}$), associated with SBS for UL transmission based on DUDe user association, is written as

$$\mathtt{C}_{\mathtt{S}}^{\mathtt{ul,DUDe}}=\tag{51}$$
$$\int_0^\infty F_{\mathtt{I}_{\mathtt{S},0}^{\mathtt{ul}}}\left(\mathtt{I}_{\mathtt{S},0}^{\mathtt{ul}}\leq\frac{\mathbb{E}\{P_{U_0}\}\beta\mathbb{E}\left\{g_0\right\}}{\gamma_{\mathtt{th}}u^{\alpha_S}}-\epsilon P_{\mathtt{RSI}}^{S}-N_0\right)f_{X_{S,0}}^{NBA}(x)dx,$$

where $f_{X_{S,0}}^{NBA}(x)$ is pdf of the distance between the typical UE and its serving SBS based on NBA scheme, $F_{\mathtt{I}_{\mathtt{S},0}^{\mathtt{ul}}}(\cdot)$ is the cdf of the interference $\mathtt{I}_{\mathtt{U}_0^{\mathtt{dl,k}}}$ and given by

$$F_{\mathtt{I}_{\mathtt{S},0}^{\mathtt{ul}}}(x)=\tag{52}$$
$$\frac{1}{2}-\frac{1}{\pi}\int_0^\infty\mathrm{Im}\left[\frac{\mathcal{L}_{\mathtt{I}_{\mathtt{M,i}}^{\mathtt{ul}}}(-jw)\cdot\mathcal{L}_{\mathtt{I}_{\mathtt{S,i}}^{\mathtt{ul}}}(-jw)\cdot\mathcal{L}_{\mathtt{I}_{\mathtt{U}}^{\mathtt{ul}}}(-jw)}{\exp\left(jw\left(\frac{\mathbb{E}\{P_{U_0}\}\beta\mathbb{E}\{g_0\}}{\gamma_{\mathtt{th}}u^{\alpha_S}}-\epsilon P_{\mathtt{RSI}}^{S}-N_0\right)\right)}\right]\frac{dw}{w},$$

where $\mathcal{L}_{\mathtt{I}_{\mathtt{M,i}}^{\mathtt{ul}}}(-jw)$, $\mathcal{L}_{\mathtt{I}_{\mathtt{S,i}}^{\mathtt{ul}}}(-jw)$, and $\mathcal{L}_{\mathtt{I}_{\mathtt{U}}^{\mathtt{ul}}}(-jw)$ are the Laplace transform of the pdf of $\mathtt{I}_{\mathtt{M,i}}^{\mathtt{ul}}$, $\mathtt{I}_{\mathtt{S,i}}^{\mathtt{ul}}$, and $\mathtt{I}_{\mathtt{U}}^{\mathtt{ul}}$, respectively. We now proceed to obtain $\mathcal{L}_{\mathtt{I}_{\mathtt{M,i}}^{\mathtt{ul}}}(-jw)$ as

$$\mathcal{L}_{\mathtt{I}_{\mathtt{M,i}}^{\mathtt{ul}}}(-jw)=\mathbb{E}\left\{e^{-(-jw)\mathtt{I}_{\mathtt{M,i}}^{\mathtt{ul}}}\right\}\tag{53}$$
$$=\mathbb{E}_{\Phi,h}\left\{\exp\left(\sum_{X_{M,i}\in\Phi_M}P_M g_{M,i}^{I}\beta\|X_{M,i}\|^{-\alpha_M}\right)\right\}$$
$$\overset{(a)}{=}\mathbb{E}_{\Phi}\left\{\prod_{X_{M,i}\in\Phi_M}\exp\left(jwP_M\beta\|X_{M,i}\|^{-\alpha_M}\right)\right\}$$
$$\overset{(b)}{=}\exp\left(-2\pi\lambda_M\int_R^\infty\left(1-\exp\left(jwP_M\beta x^{-\alpha_M}\right)\right)dx\right),$$

where (a) follows from $\mathbb{E}\left\{g_{M,i}^{I}\right\}=1$, (b) is obtained by using the PGFL of the PPP, R is the shortest distance between SBS and interfering MBS. Similarly, $\mathcal{L}_{\mathtt{I}_{\mathtt{S},\mathtt{i}}^{\mathtt{ul}}}\left(-jw\right)$ is calculated as

$$\mathcal{L}_{\mathtt{I}_{\mathtt{S},\mathtt{i}}^{\mathtt{ul}}}\left(-jw\right)=\exp\left(-2\pi\lambda_S\int_R^{\infty}\left(\frac{-jwP_S\beta x^{-\alpha_S}}{1-jwP_S\beta x^{-\alpha_S}}\right)xdx\right), \tag{54}$$

where R is the minimum distance between SBS and interfering SBSs. In addition, $\mathcal{L}_{\mathtt{I}_{\mathtt{U}}^{\mathtt{ul}}}\left(-jw\right)$ is given by

$$\exp\left(-2\pi\lambda_S\Lambda_k^i\int_0^{\infty}\left(\frac{-jw\mathbb{E}\left\{P_{U_0}\right\}\Big|_k^i\beta u^{-\alpha_S}}{1-jw\mathbb{E}\left\{P_{U_0}\right\}\Big|_k^i\beta u^{-\alpha_S}}\right)udu\right). \tag{55}$$

Finally, by substituting (53), (54), and (55) into (52), and then plugging (52) and (39) into (51), we arrive at the desired result in (27).

Appendix E
Proof of Proposition4

The UL coverage probability for a typical UE, $\mathtt{U}_0^{\mathtt{dl},\mathtt{S}}$, associated with SBS in DL and UL based on DUCo user association is evaluated following the similar steps as of Proposition 2. The pdf of the distance between $\mathtt{U}_0^{\mathtt{dl},\mathtt{S}}$ and its serving SBS is given by (38). Moreover, based on the DUCo user association, $\mathtt{U}_0^{\mathtt{dl},\mathtt{M}}$ is not operating in FD mode.

References

[1] S. Haghgoy, M. Mohammadi, and Z. Mobini, "Performance analysis of decoupled UL/DL user association in wireless-powered massive MIMO-aided heterogeneous networks," in *Proc. Int. Conf. Internet of Things and Applications (IoT)*, Isfahan, Iran, May 2021, pp. 1–7.

[2] S. Akbar, Y. Deng, A. Nallanathan, M. Elkashlan, and G. K. Karagiannidis, "Massive multiuser MIMO in heterogeneous cellular networks with full duplex small cells," *IEEE Trans. Commun.*, vol. 65, no. 11, pp. 4704–4719, Nov. 2017.

[3] J. Lee and T. Q. S. Quek, "Hybrid full-/half-duplex system analysis in heterogeneous wireless networks," *IEEE Trans. Wireless Commun.*, vol. 14, no. 5, pp. 2883–2895, May 2015.

[4] Z. Sattar, J. V. De Carvalho Evangelista, G. Kaddoum, and N. Batani, "Full-duplex two-tier heterogeneous network with decoupled access: Cell association, coverage, and spectral efficiency analysis," *IEEE Access*, vol. 8, pp. 172 982–172 995, 2020.

[5] Q. Li, S. X. Wu, S. Wang, and J. Lin, "Joint uplink/downlink discrete sum rate maximization for full-duplex multicell heterogeneous networks," *IEEE Trans. Veh. Technol.*, vol. 69, no. 3, pp. 2758–2770, Mar. 2020.

[6] M. O. Al-Kadri, Y. Deng, A. Aijaz, and A. Nallanathan, "Full-duplex small cells for next generation heterogeneous cellular networks: A case study of outage and rate coverage analysis," *IEEE Access*, vol. 5, pp. 8025–8038, 2017.

[7] F. Boccardi, J. Andrews, H. Elshaer, M. Dohler, S. Parkvall, P. Popovski, and S. Singh, "Why to decouple the uplink and downlink in cellular networks and how to do it," *IEEE Commun. Mag.*, vol. 54, no. 3, pp. 110–117, Mar. 2016.

[8] J. G. Andrews, S. Buzzi, W. Choi, S. V. Hanly, A. Lozano, A. C. K. Soong, and J. C. Zhang, "What will 5G be?" *IEEE J. Sel. Areas Commun.*, vol. 32, no. 6, pp. 1065–1082, June 2014.

[9] S. Singh, X. Zhang, and J. G. Andrews, "Joint rate and SINR coverage analysis for decoupled uplink-downlink biased cell associations in HetNets," *IEEE Trans. Wireless Commun.*, vol. 14, no. 10, pp. 5360–5373, Oct. 2015.

[10] B. Clerckx, K. Huang, L. R. Varshney, S. Ulukus, and M.-S. Alouini, "Wireless power transfer for future networks: Signal processing, machine learning, computing, and sensing," *IEEE J. Sel. Topics Signal Process.*, vol. 15, no. 5, pp. 1060–1094, Aug. 2021.

[11] H. Chen, Y. Li, J. Luiz Rebelatto, B. F. Uchôa-Filho, and B. Vucetic, "Harvest-then-cooperate: Wireless-powered cooperative communications," *IEEE Trans. Signal Process.*, vol. 63, no. 7, pp. 1700–1711, Apr. 2015.

[12] Y. Zhu, L. Wang, K. K. Wong, S. Jin, and Z. Zheng, "Wireless power transfer in massive MIMO-aided HetNets with user association," *IEEE Trans. Commun.*, vol. 64, no. 10, pp. 4181–4195, Oct. 2016.

[13] M. Mohammadi, B. K. Chalise, H. A. Suraweera, H. Q. Ngo, and Z. Ding, "Design and analysis of full-duplex massive antenna array systems based on wireless power transfer," *IEEE Trans. Commun.*, vol. 69, no. 2, pp. 1302–1316, Feb. 2021.

[14] H. Elshaer, F. Boccardi, M. Dohler, and R. Irmer, "Downlink and uplink decoupling: A disruptive architectural design for 5G networks," in *Proc. IEEE Global Commun. Conf. (GLOBECOM'14)*, Austin, TX, USA, Dec. 2014, pp. 1798–1803.

[15] M. Bacha, Y. Wu, and B. Clerckx, "Downlink and uplink decoupling in two-tier heterogeneous networks with multi- antenna base stations," *IEEE Trans. Wireless Commun.*, vol. 16, no. 5, pp. 2760–2775, 2017.

[16] C.-H. Liu and H.-M. Hu, "Full-duplex heterogeneous networks with decoupled user association: Rate analysis and traffic scheduling," *IEEE Trans. Commun.*, vol. 67, no. 3, pp. 2084–2100, Mar. 2019.

[17] K. Sun, J. Wu, W. Huang, H. Zhang, H.-Y. Hsieh, and V. C. M. Leung, "Uplink performance improvement for downlink-uplink decoupled hetnets with non-uniform user distribution," *IEEE Trans. Veh. Technol.*, vol. 69, no. 7, pp. 7518–7530, July 2020.

[18] C. DAI, K. Zhu, C. Yi, and E. Hossain, "Decoupled uplink-downlink association in full-duplex cellular networks: A contract-theory approach," *IEEE Trans. Mobile Comput.*, vol. 21, no. 3, pp. 911–925, Mar. 2022.

[19] B. Lahad, M. Ibrahim, S. Lahoud, K. Khawam, and S. Martin, "Joint modeling of TDD and decoupled uplink/downlink access in 5G HetNets with multiple small cells deployment," *IEEE Trans. Mobile Comput.*, vol. 20, no. 7, pp. 2395–2411, July 2021.

[20] Y. Shi, E. Alsusa, and M. W. Baidas, "Joint DL/Ul decoupled cell-association and resource allocation in D2D-underlay HetNets," *IEEE Trans. Veh. Technol.*, vol. 70, no. 4, pp. 3640–3651, Apr. 2021.

[21] S. Akbar, Y. Deng, A. Nallanathan, M. Elkashlan, and A. Aghvami, "Simultaneous wireless information and power transfer in K-tier heterogeneous cellular networks," *IEEE Trans. Wireless Commun.*, vol. 15, no. 8, pp. 5804–5818, Aug. 2016.

[22] L. Wang, K. Wong, R. W. Heath, and J. Yuan, "Wireless powered dense cellular networks: How many small cells do we need?" *IEEE J. Sel. Areas Commun.*, vol. 35, no. 9, pp. 2010–2024, Sept. 2017.

[23] Y. Xu, G. Li, Y. Yang, M. Liu, and G. Gui, "Robust resource allocation and power splitting in SWIPT enabled heterogeneous networks: A robust minimax approach," *IEEE Internet Things J.*, vol. 6, no. 6, pp. 10 799–10 811, Dec. 2019.

[24] H. Ma, J. Cheng, and X. Wang, "Proportional fair secrecy beamforming for MISO heterogeneous cellular networks with wireless information and power transfer," *IEEE Trans. Commun.*, vol. 67, no. 8, pp. 5659–5673, Aug. 2019.

[25] A. M. Alqasir and A. E. Kamal, "Cooperative small cell HetNets with dynamic sleeping and energy harvesting," *IEEE Trans. Green Commun. Netw.*, vol. 4, no. 3, pp. 774–782, Sept. 2020.

[26] R. Zhang, K. Xiong, W. Guo, X. Yang, P. Fan, and K. B. Letaief, "Q-learning-based adaptive power control in wireless RF energy harvesting heterogeneous networks," *IEEE Systems J.*, vol. 15, no. 2, pp. 1861–1872, 2021.

[27] B. Li, Y. Dai, Z. Dong, E. Panayirci, H. Jiang, and H. Jiang, "Energy-efficient resources allocation with millimeter-wave massive MIMO in ultra dense HetNets by SWIPT and CoMP," *IEEE Trans. Wireless Commun.*, vol. 20, no. 7, pp. 4435–4451, July 2021.

[28] I. S. Gradshteyn and I. M. Ryzhik, *Table of Integrals, Series and Products*, 7th ed. Academic Press, 2007.

[29] C. Liu and K. L. Fong, "Fundamentals of the downlink green coverage and energy efficiency in heterogeneous networks," *IEEE J. Sel. Areas Commun.*, vol. 34, no. 12, pp. 3271–3287, Dec. 2016.

[30] C. Liu and L. Wang, "Optimal cell load and throughput in green small cell networks with generalized cell association," *IEEE J. Sel. Areas Commun.*, vol. 34, no. 5, pp. 1058–1072, May 2016.

[31] C. Liu and H. Hu, "Full-duplex heterogeneous networks with decoupled user association: Rate analysis and traffic scheduling," *IEEE Trans. Commun.*, vol. 67, no. 3, pp. 2084–2100, Mar. 2019.

[32] A. H. Sakr and E. Hossain, "On user association in multi-tier full-duplex cellular networks," *IEEE Trans. Commun.*, vol. 65, no. 9, pp. 4080–4095, Sept. 2017.

[33] K. Hosseini, W. Yu, and R. S. Adve, "Large-scale MIMO versus network MIMO for multicell interference mitigation," *IEEE J. Sel. Topics Signal Process.*, vol. 8, no. 5, pp. 930–941, Oct. 2014.

[34] T. Riihonen, S. Werner, and R. Wichman, "Mitigation of loopback self-interference in full-duplex MIMO relays," *IEEE Trans. Signal Process.*, vol. 59, pp. 5983–5993, Dec. 2011.

[35] M. Mohammadi, H. A. Suraweera, Y. Cao, I. Krikidis, and C. Tellambura, "Full-duplex radio for uplink/downlink wireless access with spatially random nodes," *IEEE Trans. Commun.*, vol. 63, no. 12, pp. 5250–5266, Dec. 2015.
[36] Y. Liu, Z. Qin, M. Elkashlan, A. Nallanathan, and J. A. McCann, "Non-orthogonal multiple access in large-scale heterogeneous networks," *IEEE J. Sel. Areas Commun.*, vol. 35, no. 12, pp. 2667–2680, Dec. 2017.
[37] Z. Kuang, G. Liu, G. Li, and X. Deng, "Energy efficient resource allocation algorithm in energy harvesting-based D2D heterogeneous networks," *IEEE Internet Things J.*, vol. 6, no. 12, pp. 557–567, Feb. 2019.